Volume 2, Issue 2 – January – June-2015

E C O R F A N

# Journal-Bolivia

ISSN-On line: 2410-4191

ECORFAN®

**Indexing**

**Academic Google**

# ECORFAN-Bolivia

**ECORFAN Journal-Bolivia**, Volume 2, Issue 2, January-June 2015, is a journal edited four- monthly by ECORFAN. *21* Santa Lucía *street, Postcode: 5220.* Libertadores –*Sucre-Bolivia* WEB: www.ecorfan.org/bolivia/,journal@ecorfan.org. Editor in Chief: Ramos Escamilla- María. ISSN-On line: 2410-4191. Responsible for the latest update of this number ECORFAN Computer Unit.Escamilla Bouchán-Imelda,Luna Soto-Vladimir. *21* Santa Lucía *street, Postcode: 5220.* Libertadores -*Sucre (Bolivia)*, last updated June 30, 2015.

## Editorial Board

## Arbitration Committee

MTT, PhD.
*Universidad de Granada, Spain*

AH, PhD.
*Simon Fraser University, Canada*

AG, PhD.
*Economic Research Institute - UNAM, Mexico.*

MKJC, MsC.
*Universidad San Francisco Xavier de Chuquisaca, Bolivia*

MRCY, PhD.
*Universidad de Guadalajara, Mexico*

MEC, PhD.
*Universidad Anáhuac, Mexico*

AAB, PhD.
*Universidad Autónoma de Sinaloa, Mexico*

EDC, MsC.
*Instituto Tecnológico y de Estudios Superiores de Monterrey, Mexico*

JRB, PhD.
*Universidad Panamericana, Mexico*

AGB, PhD.
*Instituto de Biotecnología UNAM, Mexico*

ACR, PhD.
*Universidad Nacional Autónoma de México, Mexico*

ETT, PhD.
*CICATA-Instituto Politécnico Nacional, Mexico*

FVP, PhD.
GHC, PhD.
JTG, PhD.
MMG, PhD.
*Instituto Politécnico Nacional-Escuela Superior de Economía, Mexico*

FNU, PhD.
*Universidad Autónoma Metropolitana, Mexico*

## Presentation

ECORFAN Journal-Bolivia is a research journal that publishes articles in the areas of:

**E**ngineering **C**hemestry **O**ptical **R**esources **F**ood Technology **A**natomy and **N**utrition.

In Pro-Research, Teaching and Training of human resources committed to Science. The content of the articles and reviews that appear in each issue are those of the authors and does not necessarily the opinion of the editor in chief.

In Number 1st presented in Section of Engineering an article *Calculation of Dynamic Properties of Hybrid Supports of injected lubricant. Analytical Development* by RAMIREZ, Ignacio, JARAMILLO, Jesús y RECIO-CAMPOS, Celeste with adscription in the Instituto Tecnológico de Pachuca, in Section of Chemestry an article *Location Effect of Temperature Control on the Fund in a CPD* by MEDINA, Leonardo, URREA, Galo, REYNOSO, Eusebio and PLIEGO, Yolanda with adscription in the Instituto Tecnológico de Orizaba, in Section of Optical an article *Portable system for capturing images of the sclera* by ROJAS, Carlos, ROJAS, Rafael, BAUTISTA, Jorge y TRUJILLO, Valentín, in Section of Resources an article *The method of small perturbations to Calculate Stiffness and damping in a Short Chumacera* by RAMIREZ, Ignacio`, CANO, Alexis` and ANTONIO, Alberto, with adscription in the `Instituto Tecnológico de Pachuca and ``Universidad Tecnológica de la Mixteca, in Section of Food Technology an article *Evaluation of antibacterial activity of essential oil Origanum vulgare (oregano)* by SANDOVAL, Francisca, DOMINGUEZ, Maricela, CONTRERAS, Raúl and REYES, Coral, in Section of Anatomy an article *Dental Radiology processing for abscess detection* by SANCHEZ, María, MOLINAR, Jesús, VAZQUEZ, Sandra and ORDOÑEZ, Felipe, in Section of Nutrition an article *Habits of consumption of fruits and vegetables in Mexican adolescents and their relationship with eating disorder* by DÁVILA-LOAIZA, Martha Yolanda, with adscription in the Universidad de Londres.

## Content

Article **ECORFAN Journal**

**Engineering** June 2015 Vol.2 No.2 80-91

# Calculation of Dynamic Properties of Hybrid Supports of injected lubricant. Analytical Development

RAMIREZ, Ignacio*†, JARAMILLO, Jesús y RECIO-CAMPOS, Celeste

*Instituto Tecnológico de Pachuca. División de Estudios de Posgrado e Investigación. Carretera México-Pachuca Km 87.5, Col. Venta Prieta, Pachuca de Soto, Hidalgo. MEXICO. Teléfono (771) 711 3140, extensión 139*

Received January 8, 2014; Accepted June 12, 2015

## Abstract

In this work we obtain analytical expressions for the calculation of the stiffness and damping of a short journal bearing, which is being submitted to an external pressurization force. These expressions are obtained from Reynolds equation, which is modified to model the effect of pressurization. Such modification lies in the introduction of a generalized function of the space impulse type (Dirac Delta). It is important to mention that such modeling is first in its kind to solve rotodynamic problems. Additionally there are graphics showing the performance of the stiffness and damping coefficients as a function of the eccentricity and/or externalpressurization. It is important to notice that this is the first work that reports analytical results of such coefficients being modified by the effect of pressurization; currently there are only numerical solutions for its calculation. Also, the dynamic behavior of a rotatory system is highly influenced by the values that may be taken by the coefficients of stiffness and damping; therefore, if the dependence to pressurization is known, it is possible to determine the pressure values that may be applied until instability is reached

**Bearing, Pressurization, Coefficients Rotodynamic, Stiffness, Damping.**

**Citation:** RAMIREZ, Ignacio, JARAMILLO, Jesús y RECIO-CAMPOS, Celeste. Calculation of Dynamic Properties of Hybrid Supports of injected lubricant. Analytical Development. ECORFAN Journal-Bolivia 2015, 2-2: 80-91

* Correspondence to Author (email: tijonov@hotmail.com)
† Researcher contributing first author.

## Introduction

The equations of motion of rotor-bearings, system contain coefficients corresponding to the film of the lubricant of the bearings, these parameters change with the rotational speed and consequently also change with the addition of external pressure. That's why the dynamic behavior is always heavily influenced by the values they can take these coefficients. It is in the literature as the operation speed increases, one of the stiffness coefficients can take negative values depending on its magnitude and the system could instability [1].

To study the behavior of the fluid in the hydrodynamic bearings Reynolds equation is used, which is a simplification of the Navier-Stokes equations for Newtonian fluids type. Reynolds equation relates the fluid pressure in the bearing with axial and circumferential coordinates, so that using this equation; it is possible to obtain the pressure field. Unable to resolve analytically Reynolds equation, but can be obtained depending on the ratio approaches. (L / D); which indicates whether the bearing is short or long. Therefore, if the Reynolds equation is modified by a generalized function of spatial impulse (Dirac) that models the external lubricant injection, be possible to find an expression that determines the pressure field in the fluid film as a function of pressurizing external and in turn determine the stiffness and damping forces and corresponding coefficients, also called coefficients rotordynamic.

## Classic definition of the aerodynamic coefficients

The model describing the function of pressure in hydrodynamic bearings is the Reynolds equation, such an equation can be written generally as [2]:

$$\frac{\partial}{\partial\theta}\left[h^3\frac{\partial p}{\partial\theta}\right]+R^2\frac{\partial}{\partial z}\left[h^3\frac{\partial p}{\partial z}\right]=12\frac{\mu R^2}{C_r^2}\left[C_1\varepsilon Cos\theta+C_2\varepsilon(\varphi-\frac{\omega}{2})Sen\theta\right] \quad (1)$$

$$-\frac{L}{2}\le z\le\frac{L}{2},\quad 0\le\theta\le 2\pi,\quad h(\theta)=1+\varepsilon Cos\theta \quad (2)$$

$$p(\frac{L}{2})=0;\ p(-\frac{L}{2})=0;\ p(\theta+2\pi)=p(\theta) \quad (3)$$

Where $p:$ is the pressure in the lubricant film, $h:$ is the dimensionless film thickness of the fluid, $R:$ is the radius of the bearing represents the radial course, $C_r:$ is the bearing length, $L:$ is the equilibrium angle (attitud), $\varphi:$ is the dimensionless eccentricity of the bearing $\varepsilon:$ is the lubricant viscosity fluid, $\mu:$ is the angular coordinate in any point of the bearing and the axial coordinate of the bearing.

To work in general, it is possible dimensionless Reynolds equation using the following substitutions:

$$z=\frac{L}{2}\bar{z}\qquad p=\mu N\left(\frac{R}{Cr}\right)^2\bar{p}$$

$$N=\frac{\omega}{2\pi}\qquad \hat{p}=\frac{\bar{p}}{(1-2\dot{\varphi}/\omega)} \quad (4)$$

Then leaving:

$$\frac{\partial}{\partial\theta}\left[h^3\frac{\partial\hat{p}}{\partial\theta}\right]+\left(\frac{D}{L}\right)^2\frac{\partial}{\partial\bar{z}}\left[h^3\frac{\partial\hat{p}}{\partial\bar{z}}\right]=24\pi\frac{\dot{\varepsilon}/\omega}{(1-2\dot{\varphi}/\omega)}Cos\theta-12\pi\varepsilon Sen\theta \quad (5)$$

However, in this work the main interest is in short bearings, which comply with the condition: $L/D<1/2$.

For both the first member of (5), the first term is small compared to the second and so dimensionless Reynolds equation for short bearings remain as:

ISSN-On line: 2410-4191

$$\left(\frac{D}{L}\right)^2 \frac{\partial}{\partial \bar{z}}\left[h^3 \frac{\partial \hat{p}}{\partial \bar{z}}\right] = 24\pi \frac{\dot{\varepsilon}/\omega}{(1-2\dot{\varphi}/\omega)} Cos\theta - 12\pi\varepsilon Sen\theta \quad (6)$$

Once resolved (6), the dimensional components of force in the radial and transverse directions are:

$$\bar{F}_R = \frac{F_R}{\mu NLD(R/C_r)^2} = (1-2\dot{\varphi}/\omega) f_R \quad (7)$$

$$\bar{F}_T = \frac{F_T}{\mu NLD(R/C_r)^2} = (1-2\dot{\varphi}/\omega) f_T \quad (8)$$

$$f_R = \frac{1}{4}\int_{-1}^{1}\int_{0}^{\pi} \hat{p}(\theta,\bar{z}) Cos\theta \, d\theta \, d\bar{z} \quad (9)$$

$$f_T = \frac{1}{4}\int_{-1}^{1}\int_{0}^{\pi} \hat{p}(\theta,\bar{z}) Sen\theta \, d\theta \, d\bar{z} \quad (10)$$

The following expression relates the resultant force $f_R$ and $f_T$ to obtain a very important dimensionless number in rotodynamic:

$$S = \frac{1}{\sqrt{f_R^2 + f_T^2}} = \frac{\mu NLD}{W}\left(\frac{R}{C_r}\right)^2 = \frac{F_{\dim}}{W} \quad (11)$$

This number is called Sommerfeld number and the geometrical characteristics relating lubricant viscosity and the bearings of the hydrodynamic forces and weight.

The change of forces fR and fT around the equilibrium position provides stiffness and damping coefficients, which are defined by [3]:

$$\bar{K} = \begin{pmatrix} \frac{\partial f_R}{\partial \varepsilon} & \frac{\partial f_R}{\varepsilon \partial \varphi} - \frac{f_T}{\varepsilon} \\ \frac{\partial f_T}{\partial \varepsilon} & \frac{\partial f_T}{\varepsilon \partial \varphi} + \frac{f_R}{\varepsilon} \end{pmatrix} = \begin{pmatrix} K_{RR} & K_{RT} \\ K_{TR} & K_{TT} \end{pmatrix}$$

$$\bar{C} = \begin{pmatrix} \frac{\partial f_R}{\partial(\dot{\varepsilon}/\omega)} & -\frac{2 f_R}{\varepsilon} \\ \frac{\partial f_T}{\partial(\dot{\varepsilon}/\omega)} & -\frac{2 f_T}{\varepsilon} \end{pmatrix} = \begin{pmatrix} C_{RR} & C_{RT} \\ C_{TR} & C_{TT} \end{pmatrix} \quad (12)$$

(13)

Where $[\bar{K}]$ It is the matrix of the coefficients of stiffness and $[\bar{C}]$ is the matrix of coefficients buffer. These coefficients are related to its dimensional part by:

$$\bar{K}_{ij} = \left[\frac{C_r}{\mu NLD\left(R/C_r\right)^2}\right] K_{ij}$$

$$\bar{C}_{ij} = \left[\frac{\omega C_r}{\mu NLD\left(R/C_r\right)^2}\right] C_{ij} \quad (14)$$

Note that the thermodynamic coefficients given by (12) and (13) are referred to the system of radial and transverse coordinates, if you wanted to obtain these coefficients with respect to another coordinate system is only necessary to multiply by the corresponding rotation matrix.

Generally the coefficients of stiffness and damping are presented in the literature as:

$$\tilde{K}_{ij} = \left(\frac{C_r}{W}\right) K_{ij}$$

$$\tilde{C}_{ij} = \left(\frac{\omega C_r}{W}\right) C_{ij} \quad (15)$$

The relationship between (14) and (15) is through the Sommerfeld number given by (11) where:

$$\tilde{K}_{ij} = S\bar{K}_{ij}$$

$$\tilde{C}_{ij} = S\bar{C}_{ij} \quad (16)$$

ISSN-On line: 2410-4191

### Solution for short bearings

### External no pressurization

The mathematical model of a short bearing without external pressurization is given by (6) where the solution comes by:

$$\hat{p}=\left(\frac{L}{D}\right)^2\frac{6\pi\left(1-\bar{z}^2\right)}{\left(1+\varepsilon Cos\theta\right)^3}\left[\varepsilon Sen\theta-2\frac{\dot{\varepsilon}/\omega}{\left(1-2\dot{\varphi}/\omega\right)}Cos\theta\right] \tag{17}$$

Substituting (17) into (9) and (10), it is known that the dimensionless forces are:

$$f_R=\left(\frac{L}{D}\right)^2\left\{\frac{-4\pi\varepsilon^2}{\left(1-\varepsilon^2\right)^2}-\frac{2\pi^2\left(1+2\varepsilon^2\right)}{\left(1-\varepsilon^2\right)^{5/2}}\cdot\frac{\dot{\varepsilon}/\omega}{\left(1-2\dot{\varphi}/\omega\right)}\right\} \tag{18}$$

$$f_T=\left(\frac{L}{D}\right)^2\left\{\frac{\pi^2\varepsilon}{\left(1-\varepsilon^2\right)^{3/2}}+\frac{8\pi\varepsilon}{\left(1-\varepsilon^2\right)^2}\cdot\frac{\dot{\varepsilon}/\omega}{\left(1-2\dot{\varphi}/\omega\right)}\right\} \tag{19}$$

Thus, it is possible to find the coefficients of stiffness and damping in the radial and transverse directions of a short bearing no pressurization, only substituting (18) and (19) (12) and (13). After multiplying by the corresponding rotation matrix and using (16), the coefficients are obtained in the rectangular coordinate system. See Table 1.

| | |
|---|---|
| $\tilde{k}_{xx}=\frac{4\left[\pi^2+\left(32+\pi^2\right)\varepsilon^2+2\left(16-\pi^2\right)\varepsilon^4\right]}{\left(1-\varepsilon^2\right)\left[\pi^2+\left(16-\pi^2\right)\varepsilon^2\right]^{3/2}}$ | $\tilde{c}_{xx}=\frac{2\pi\left[\pi^2+2\left(24-\pi^2\right)\varepsilon^2+\pi^2\varepsilon^4\right]}{\varepsilon\sqrt{1-\varepsilon^2}\left[\pi^2+\left(16-\pi^2\right)\varepsilon^2\right]^{3/2}}$ |
| $\tilde{k}_{xy}=\frac{\pi\left[\pi^2+\left(32+\pi^2\right)\varepsilon^2+2\left(16-\pi^2\right)\varepsilon^4\right]}{\varepsilon\sqrt{1-\varepsilon^2}\left[\pi^2+\left(16-\pi^2\right)\varepsilon^2\right]^{3/2}}$ | $\tilde{c}_{xy}=\frac{8\left[\pi^2+2\left(\pi^2-8\right)\varepsilon^2\right]}{\left[\pi^2+\left(16-\pi^2\right)\varepsilon^2\right]^{3/2}}$ |
| $\tilde{k}_{yx}=\frac{\pi\left[-\pi^2+2\pi^2\varepsilon^2+\left(16-\pi^2\right)\varepsilon^4\right]}{\varepsilon\sqrt{1-\varepsilon^2}\left[\pi^2+\left(16-\pi^2\right)\varepsilon^2\right]^{3/2}}$ | $\tilde{c}_{yx}=\frac{8\left[\pi^2+2\left(\pi^2-8\right)\varepsilon^2\right]}{\left[\pi^2+\left(16-\pi^2\right)\varepsilon^2\right]^{3/2}}$ |
| $\tilde{k}_{yy}=\frac{4\left[2\pi^2+\left(16-\pi^2\right)\varepsilon^2\right]}{\left[\pi^2+\left(16-\pi^2\right)\varepsilon^2\right]^{3/2}}$ | $\tilde{c}_{yy}=\frac{2\pi\left(1-\varepsilon^2\right)^{1/2}\left[\pi^2+2\left(\pi^2-8\right)\varepsilon^2\right]}{\varepsilon\left[\pi^2+\left(16-\pi^2\right)\varepsilon^2\right]^{3/2}}$ |

**Table 1** Aerodynamic coefficients of stiffness and damping for short bearings in the XY system

### With external pressurization

Now you need to enter the external pressurization effect and is important to specify the axial and circumferential injection point. This article is modeled using external pressurization function space Delta Dirac impulse $\delta(x)$ (also called generalized function or distribution), which has special properties that help in solving the model.

Suppose the pressurization will be given a mathematical point that such behavior is modeled perfectly by the pulse function. This can be generalized for injections "n" arbitrary points of the bearing. Therefore, it is possible to consider incorporating the Dirac impulse function as a way to represent the lubricant injection is performed at an arbitrary position [4].

Then the bearing undergoing pressurization, performed in an injection port which axial and circumferential location is arbitrary occurs. See Figure 1.

ISSN-On line: 2410-4191

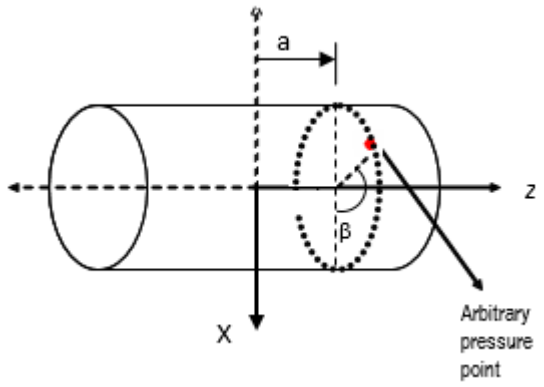


**Graphic 1** Location pressurization point in the bearing. Note that the values of the axial and circumferential coordinates to specify the particular point injection lubricant defined.

This case corresponds to pressurizing with timely door on the point with the dimensionless axial coordinate $\bar{z} = a$ and the circumferential coordinate "$\beta$",it is noteworthy that the position of the injection port can be as arbitrary as you like for any securities of "$a$" and "$\beta$" it is noteworthy That the position of the injection port can be as arbitrary as you like for any securities of

$$(\Delta\bar{p})_{prt} = \bar{q}_{prt}\,\delta(\bar{z}-a)\,\delta\left[\theta-(\pi+\beta-\varphi_{pres})\right] \qquad (20)$$

$$\bar{q}_{prt} = \frac{\Delta F_{pres}}{DL\mu N\left(R/Cr\right)^2} = \frac{\Delta F_{pres}}{F_{\dim}}$$

Note that although the Dirac delta function is defined as infinite impulse at the point of the axial and angular coordinates, the pressurizing force is not equal to infinity since as the injection port is considered a mathematical point, the product of pressure ( $\bar{q}_{prt} \to \infty$)the gate area ($\bar{A}_{prt} \to 0$) It will be a constant value.

Equally worth mentioning that the Dirac function in this model does not indicate that the pressure is applied and disappears at a certain time, is it is not a temporary role but is a spatial function for a given value axial and angular coordinate, pressure is applied in pulse form.

It is proposed as the model of pressurization in the spot port, the dimensionless equation:

$$\frac{\partial}{\partial\bar{z}}\left[h^3\frac{\partial\hat{p}}{\partial\bar{z}}\right] = \left(\frac{L}{D}\right)^2 \bar{q}_{prt}\,\delta(\bar{z}-a)\,\delta\left[\theta-(\pi+\beta-\varphi_{pres})\right]\cdot\frac{1}{\left(1-2\dot{\varphi}/\omega\right)}$$

$$\hat{p}(\bar{z}=\pm1)=0\,,\quad \hat{p}(\theta+2\pi)=\hat{p}(\theta)$$

$$-1\le\bar{z}\le1,\quad 0\le\theta\le2\pi \qquad (21)$$

Solving to (21) and using the properties of the Dirac delta function is obtained:

$$\hat{p}_{PRES} = \left(\frac{L}{D}\right)^2 \bar{q}_{prt}\,\frac{\delta\left[\theta-(\pi+\beta-\varphi_{pres})\right]}{2\left(1+\varepsilon_{pres}Cos\theta\right)^3}\left[1-a\bar{z}-|\bar{z}-a|\right]\cdot\frac{1}{\left(1-2\dot{\varphi}/\omega\right)} \qquad (22)$$

After replacing (22) in (9) and (10) yields:

$$f_R = -\left(\frac{L}{D}\right)^2 \bar{q}_{prt}\,\frac{\left(1-a^2\right)}{8}\,\frac{Cos(\beta-\varphi)}{\left[1-\varepsilon Cos(\beta-\varphi)\right]^3}\cdot\frac{1}{\left(1-2\dot{\varphi}/\omega\right)} \qquad (23)$$

$$f_T = -\left(\frac{L}{D}\right)^2 \bar{q}_{prt}\,\frac{\left(1-a^2\right)}{8}\,\frac{Sen(\beta-\varphi)}{\left[1-\varepsilon Cos(\beta-\varphi)\right]^3}\cdot\frac{1}{\left(1-2\dot{\varphi}/\omega\right)} \qquad (24)$$

Substituting (23) and (24) (12) and (13) and after multiplication by the corresponding rotation matrix, the coefficients rotordynamic due to pressurization are obtained. See Table 2.

ISSN-On line: 2410-4191

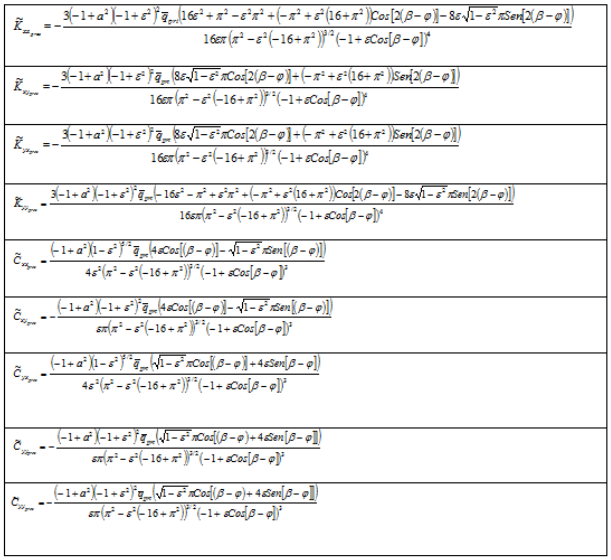

**Table 2** Aerodynamic Coefficients stiffness and damping of a short bearing due to external pressurization arbitrary circumferential and axial positions.

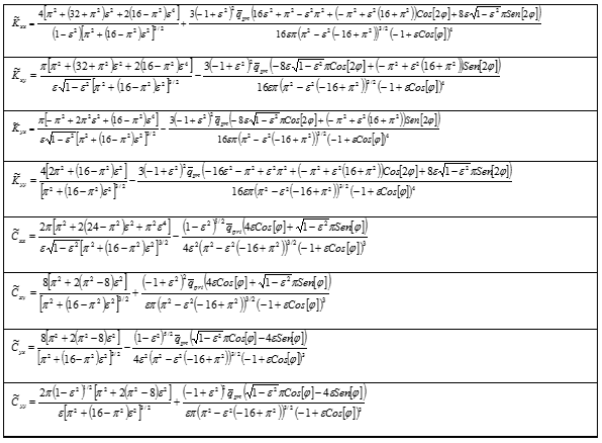

**Table 3** Aerodynamic Coefficients complete table of stiffness and damping of pressurized bearing on their part

**Table 4** Aerodynamic Coefficients complete table of stiffness and damping of pressurized bearing its top center

## Classic case

In the following figures, the conduct of rotordynamic coefficients as a function of the eccentricity of equilibrium for different values of external pressurization force is shown.

Important Note: The dotted lines indicate negative values

**1.-** $f_{prt} = 0$

When the pressurizing force is zero, is obtained the classic case of the coefficients reported in the literature [2]. In Figures 2 and 3 the rotordynamic coefficients for this case (direct and coupled) appear. Mentioned coefficients were obtained from the formulas given in Table 1, for a short bearing unpressurized externally.

ISSN-On line: 2410-4191

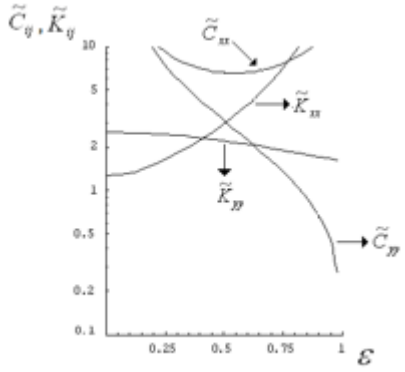


**Graphic 2** Direct Aerodynamic coefficients of stiffness and damping for a short bearing unpressurized. $f_{prt} = 0$.

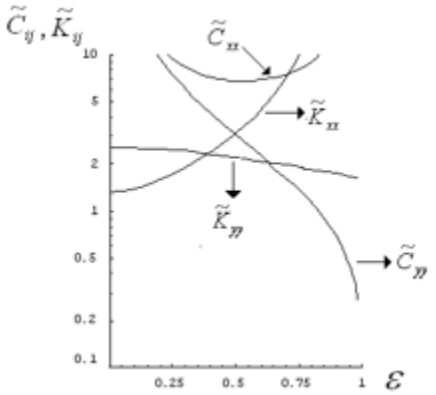


**Graphic 3** Coupled Aerodynamic coefficients of stiffness and damping for a short bearing unpressurized. $f_{prt} = 0$.

**Pressurized case (Y).**

Below the graphs the coefficients of stiffness and damping for different values presented pressurizing force, the above is obtained from the formulas found in Tables 3 and 4.

**Lower injection**

**2.-** $f_{prt} = 10$

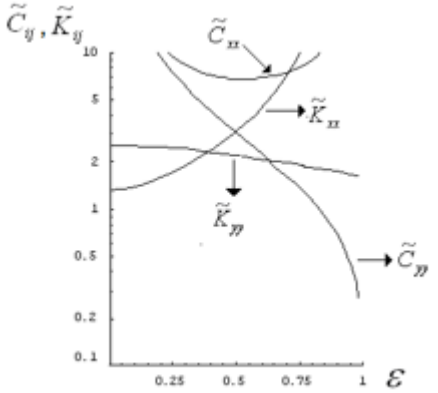


**Graphic 4** Direct Aerodynamic coefficients of stiffness and damping for a short bearing pressurized at the bottom. $f_{prt} = 10$.

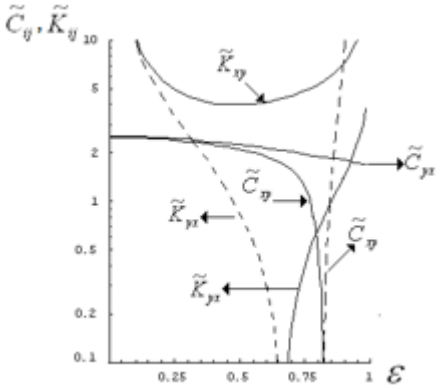


**Graphic 5** Aerodynamic Coefficients of Coupled stiffness and damping for a short bearing pressurized at the bottom. $f_{prt} = 10$.

Importantly, Figures 4 and 5, the pressurization causes significant changes only in the coefficients for the vertical directions $\tilde{K}_{xx}, \tilde{C}_{xx}$ and the values of the damping in the directions $\tilde{C}_{xy}$, where not only a separation appears with the coefficient $\tilde{C}_{yx}$ (as it was in Figure 3) but also show negative values for certain ranges of eccentricity, so that they can affect the stability of the system.

In figures 6 through 9 behavior occurs when coefficients rotor dynamic further increases the pressurizing force at the bottom of the bearing.

ISSN-On line: 2410-4191

Note that the graph of damping coefficient $\tilde{C}_{xy}$ (with corresponding negative signs) is going farther and farther to the left for different values of pressurization (Figs. 7 and 9).

**3.-** $f_{prt} = 100$

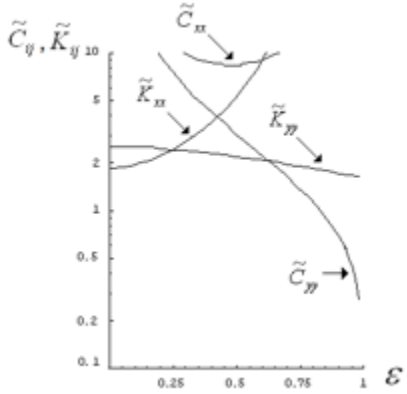


**Graphic 6** Direct Aerodynamic coefficients of stiffness and damping for a short bearing pressurized at the bottom. $f_{prt} = 100$.

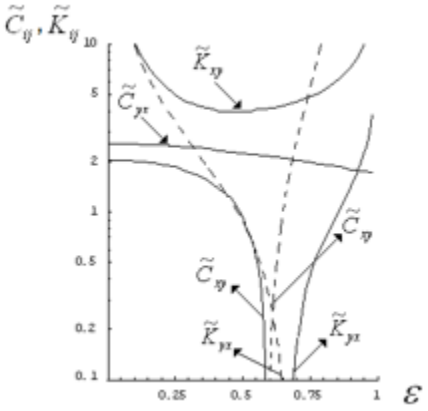


**Graphic 7** Aerodynamic Coefficients of Coupled stiffness and damping for a short bearing pressurized at the bottom. $f_{prt} = 100$.

**4.-** $f_{prt} = 500$

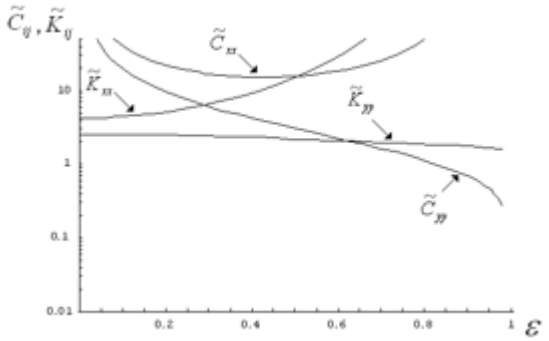


**Graphic 8** Aerodynamic coefficients of stiffness and damping for a short bearing pressurized at the bottom. $f_{prt} = 500$.

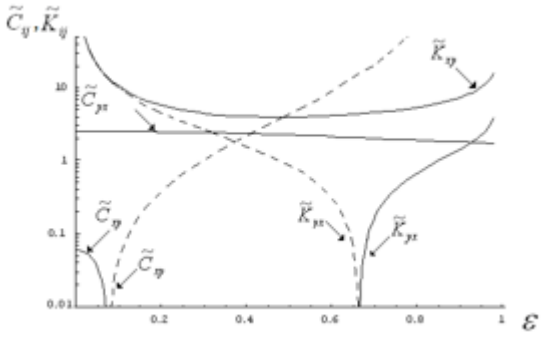


**Graphic 9** Coupled Aerodynamic coefficients of stiffness and damping for a short bearing pressurized at the bottom. $f_{prt} = 500$.

## Comparison of aerodynamic coefficients (Lower injection)

The following figures show the comparison of rotor dynamic stiffness and damping coefficients (direct in the direction xx) and the buffer (coupled in the x direction) for different values of pressurizing force. Remember that these coefficients are modified to look more drastically when are pressurized externally to the bearing.

Figures 10, 11, 12 and 13 show that the values of stiffness and damping direct in the vertical direction of the lubricant film increases with increasing the strength of external pressurization.

ISSN-On line: 2410-4191

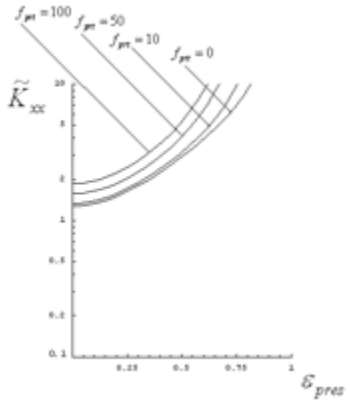


**Graphic 10** Comparison of direct aerodynamic coefficients (in the vertical direction) of a short bearing rigidity for different pressurization values bottom.

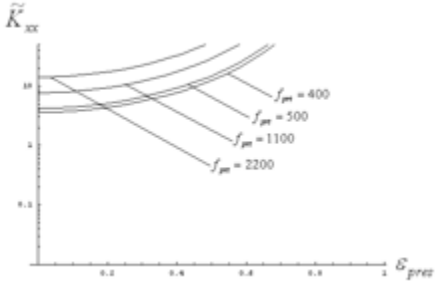


**Graphic 11** Direct comparison of aerodynamic coefficients (in the vertical direction) of a short bearing rigidity for different pressurization values bottom.

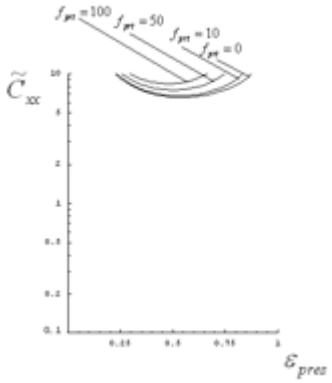


**Graphic 12** Direct comparison of aerodynamic coefficients (in the vertical direction) damping of a short bearing for different pressurization values bottom.

Figures 14 and 15 show that as the strength of external pressurization, the damping coefficient in the x direction begins to change sign for certain values of eccentricity and therefore tend to be traveled curves to the left, until it stops values over pressurizing the damping coefficient becomes negative for all possible values of eccentricity, doing this may affect significantly to system stability manner.

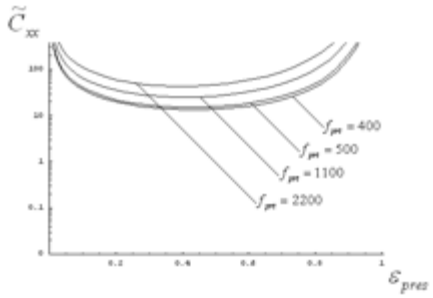


**Graphic 13** Comparison of direct rotor dynamic coefficients (in the vertical direction) damping of a short bearing for different pressurization values bottom.

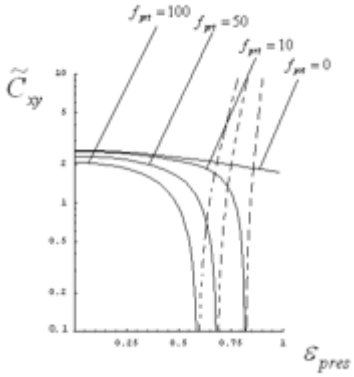


**Graphic 14** Comparison of coupled rotor dynamic coefficients (in the x direction) damping of a short bearing for different pressurization values bottom.

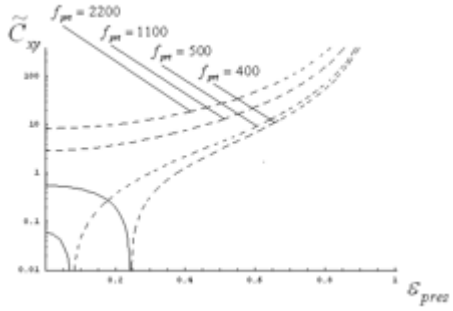


**Graphic 15** Comparison of coupled rotor dynamic coefficients (in the x direction) damping of a short bearing for different pressurization values bottom.

ISSN-On line: 2410-4191

**Pressurized case (ii)**

**Superior injection**

The following graphic shows this variation for different values of pressurizing force, on top of the bearing.

**1.-** $f_{prt} = 10$

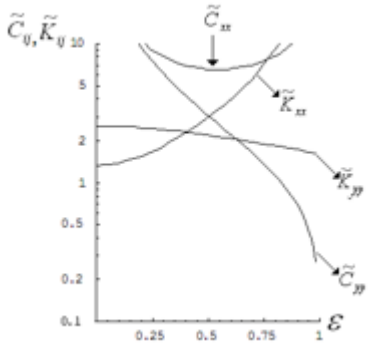

**Graphic 16** Direct Rotor dynamic coefficients of stiffness and damping for a short pressurized bearing at the top. $f_{prt} = 10$

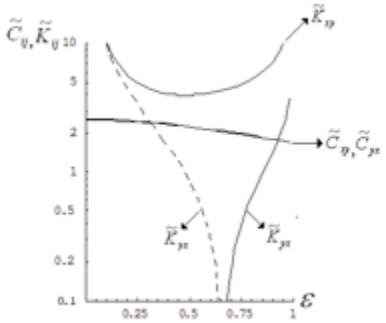

**Graphic 17** Rotor dynamic Coefficients of Coupled stiffness and damping for a short pressurized bearing at the top. $f_{prt} = 10$.

As in the previous case (lower injection), the rotor dynamic coefficients are considerably affected are primarily direct in the vertical direction and the buffer $\tilde{C}_{xy}$; which unlike the previous case, it is not negative for any value of eccentricity.

**2.-** $f_{prt} = 100$

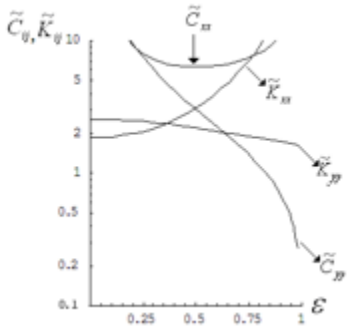

**Graphic 18** Direct rotor dynamic coefficients of stiffness and damping for a short pressurized bearing on its top. $f_{prt} = 100$.

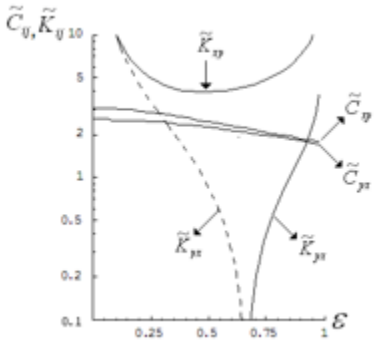

**Graphic 19** Rotor dynamic Coefficients of Coupled stiffness and damping for a short pressurized bearing at the top. $f_{prt} = 100$.

## Comparison of Rotor dynamic coefficients (Superior Injection)

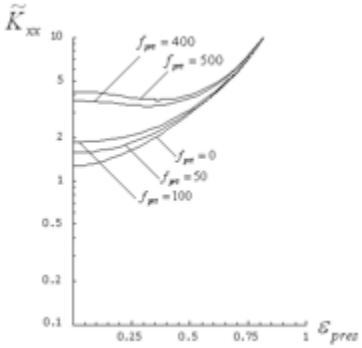

**Graphic 20** Comparison of direct rotor dynamic coefficients (in the vertical direction) of a short bearing rigidity for different values of pressurization at the top.

ISSN-On line: 2410-4191

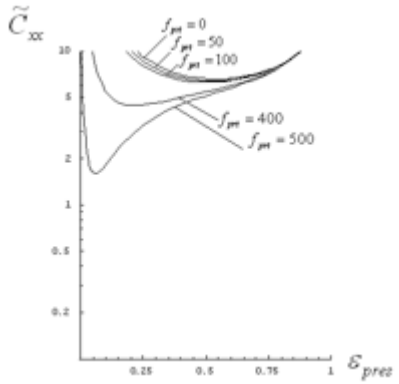


**Graphic 21** Comparison of direct rotor dynamic coefficients (in the vertical direction) damping of a short bearing for different values of pressurization at the top.

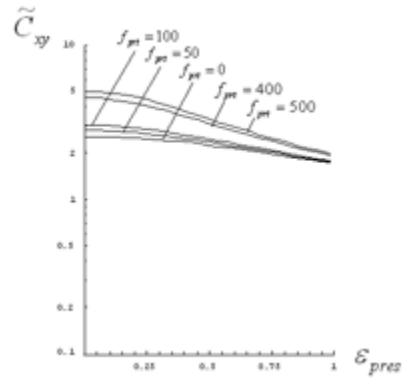


**Graphic 22** Comparison of coupled rotor dynamic coefficients (in the x direction) damping of a short bearing for different values of pressurization at the top.

## Conclusions

The results found in this work are of fundamental importance, since it was obtained for the first time in international and analytically literature, rotor dynamic coefficients of stiffness and damping as a function of the strength of external pressurization (are summarized in Tables 2 , 3 and 4).

Currently only numeric values of these coefficients are making it less manageable the results; This was possible by using the Dirac external effect pressurization as in equation Reynolds lubrication spatial function.

Graphics behaviors rotor dynamic pressurized coefficients as a function of the eccentricity of balance and pressurizing force in cases where it is pressurized at the bottom and top of the bearing found.

When is pressurized at the bottom, we find that the coefficients of stiffness and direct buffer (in the vertical direction) increase in value as the external pressurizing force is growing, just as the damping coefficient in the x direction is affected in their values when pressurization grows, including changes sign for certain values of eccentricity; This result is of fundamental importance for the stability of the system is determined by the values rotor dynamic having such coefficients, being more conducive to instability as these coefficients take negative values.

Moreover when pressurized at the top of the bearing, the values of the stiffness (in the vertical direction) increase in value as it grows pressurization, but now the damping in the vertical direction decreases when the pressing force grows . Similarly, the damping coefficient in the x direction increases to values greater than the pressing force.

## Referencies

A. Antonio García, V. Nosov, J. Gómez Mancilla (2002) "Comparación de coeficientes Rotodinámicos de chumaceras hidrodinámicas usando la teoría de chumaceras a largas, cortas y Warner" 3° Congreso Internacional de Ingeniería Electromecánica y de Sistemas IPN.

Childs, D., (1993)"Turbomachinery Rotor dynamics: Phenomena, Modeling,& Analysis," John Wiley&Sons, NY.

Szeri. (1998) Fluid Film Lubricatión. Theory and Design Cambridge University Press.

ISSN-On line: 2410-4191

V. Nosov, I. Ramírez Vargas, J. Gómez Mancilla (2005). "New model and Stationary Position for a Short Journal Bearings with Point Injection Ports". To be evaluate in the Journal of Turbomachinery.

I. Ramirez Vargas, V.R.Nosov, J. Gómez Mancilla (2004). "Campos de presión de lubricante en chumacera híbrida presurizada con anillo y/o línea unidimensional de presurización", 8° Congreso Nacional de Ingeniería Electromecánica y de Sistemas IPN

Bently D, Petchnev (2000) "Dynamic stiffness and advantages of externally pres-surized fluid film bearings", Orbit, First Quarter.

Khonsari, M.M., Booser, E.R. (2001) "Applied Tribology: Bearing Design and Lubrication," John Wiley & Sons.

Arfken (2000), Mathematical Methods for Physic, AcademicPress 5ta Ed.

ISSN-On line: 2410-4191

Article ECORFAN Journal
Chemestry June 2015 Vol.2 No.2 92-100

# Location Effect of Temperature Control on the Fund in a CPD

MEDINA, Leonardo*†, URREA, Galo, REYNOSO, Eusebio and PLIEGO, Yolanda

*División de Estudios de Posgrado e Investigación, Instituto Tecnológico de Orizaba. Av. Instituto Tecnológico No. 852, C.P. 94320, Orizaba, Ver. México*

Received January 8, 2014; Accepted June 12, 2015

## Abstract

In this work the effect of the location of the secondary loop temperature control on the performance of a structure to control product composition background of a dividing wall column (DWC) is studied. The results show that the location has a significant effect in the control and in proper positions is possible to maintain product purity background close to the desired value in the presence of disturbances in the feed composition. The backstepping methodology shows the nature of the design temperature-temperature cascade control, in addition to extensions multicascada obtained control. Based on these initial results it will be possible to obtain control structures based on multiple temperature measurements for controlling the composition of the products in dividing wall columns making a contribution to the research of control in this type of separation structure.

**Column, distillation, control, disturbances**

**Citation:** MEDINA, Leonardo, URREA, Galo, REYNOSO, Eusebio and PLIEGO, Yolanda. Location Effect of Temperature Control on the Fund in a CPD. ECORFAN Journal-Bolivia 2015, 2-2: 92-100

* Correspondence to Author (email: itorizaba@hotmail.com)
† Researcher contributing first author.

## Introduction

Distillation is the separation process more common in the chemical process industry. Usually a ternary mixture can be separated by a direct, indirect or a distributed sequence comprising two or three distillation columns. It has made a significant effort in developing new methods of design, optimization and control of thermally coupled distillation columns, which provide savings of up to 30% of the annual cost in the separation compared to conventional distillation sequences ( Schultz et al., 2002). To reduce the number of columns and avoid remixing in such sequences, a thermally coupled arrangement that is now known as Petlyuk distillation column (Figure 1a) and in it the vapor streams and liquid exiting from the prefractionator introduced They are directly connected with a second column directly eliminating a column, a reboiler and a condenser. An alternative configuration for the prefractionator thermally coupled using a single housing with a vertical partition dividing the central section of the housing into two parts is known as dividing wall column (CPD) (Figure 1b).

Despite the potential benefits of the dividing wall column, it was not until in recent years the industry chosen by them (Kaibel, 2002). The main reason for the slow acceptance is attributed to lack of knowledge on the dynamics of the process and its controllability (Abdul Muttalib et al, 1998a;. Abdul Muttalib et al, 1998b;. Serra et al., 2003). Recently there has been more effort on these issues and have been published more articles on the dynamics, control and operation of dividing wall columns (Rodriguez and Chinea, 2012).

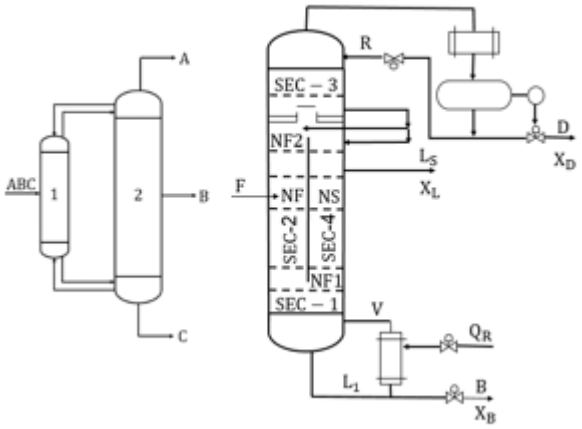


**Figure 1** Column Petlyuk (a) Dividing Wall Column (b)

Because the temperature measurements are usually more sensitive and cheaper than compositional schemes have been proposed inferential control these measurements. Luyben 1969 proposes a technique to control the product composition of a distillation column by controlling the difference between two temperature differences (DT) column. Raised as an effective control scheme for a variety of disturbances in different operating conditions such as disturbances in the feed rate and feed compositions, achieving better performance on the grounds that the changes are canceled in the pressure drop if two (DT) are taken in the same section of the column where the same changes are in the vapor and liquid loads. In 1996, Wolff Skogestad and present examples of the application of cascade control for distillation columns to quantify improvements focusing on the interaction and the rejection of disturbances and provide some analytical expressions for the gain of the secondary controller. Shin et al. (2000) proposed an observer using temperature measurements of plates instead of the composition. Ling and Luyben (2010) made attempts to control the composition indirectly to the operation of the DWC and these include structures for temperature control (TC) and control of temperature difference (TDC).

ISSN-On line: 2410-4191

Luan et al. (2013) proposed a control structure simple temperature difference (STDC), consisting of two temperatures and two control loops temperature difference.

Cascade control applied to distillation columns possesses robustness properties is still not entirely clear, however, Alvarez-Ramirez et al. (2002) used the backstepping approach where passivation show that the nature of the design of cascade control of the composition in a distillation column is rinsed under these terms, plus systematic extensions for configuration control is obtained as multicascada a natural consequence of this same design. These researchers used a cascade control composition-temperature, however in controlling the composition by measuring the composition often presents certain practical difficulties.

Preliminary work such as Matla-González et al. (2013) and Castellanos-Sahagun and Alvarez (2013) used temperature-cascade control temperature to indirectly control the purity of the products. Early investigators apply them to a Petlyuk column consisted of linear models showing interesting input-output stability properties and performance during periods of time to disturbances in the feed composition. The second researchers applied to a binary distillation column using a combination of the theory of nonlinear constructive passivation control and observability notions.

In a previous study Medina-Rodriguez et al. (2015) designed controllers cascade temperature-temperature under the backstepping principle for rectifying section (SEC-3) of a dividing wall column evaluating the effect of the location of the temperature measurement on the performance of the controller using as manipulated variable reflux rate.

These paper controllers are designed under the same principle backstepping to the stripping section (SEC-1) of a CPD, evaluating the effect of the location of the temperature measurement on the controller performance using the rate of heat as manipulated variable.

**Dynamic Simulation System**

The dynamic behavior of the dividing wall column (CPD) is based on a dynamic model solution obtained by mass and energy balances for each component in each dish and, in thermodynamic relations. The model consists of the following set of ordinary differential equations (ODE) and algebraic equations for each stage of the column: NC-1 continuity equations for component 1 equation total continuity, one equation of energy balance, 1 Hydraulic connection for flow rates of liquid on each tray, one equation for the density of the liquid, two equations to obtain the enthalpy (liquid and vapor); NC relations vapor-liquid equilibrium. For PCD considered in this work consisted of a total of 70 stages (in the prefractionator 24 and 44 in the main column), a condenser and a reboiler, the resulting pattern was formed with a total of 280 490 ODEs and algebraic equations. The set of ordinary differential equations are solved using the Runge-Kutta algorithm 4th order.

**System Overview**

As case study considering the separation of a mixture of benzene (B), toluene (T) and o-xylene (X) which has a feed composition of 30/30/40% mol respectively and to be separated reaching individual purity of 99 mol% in the currents of distillate, intermediate and bottom. Table 1 shows the operating conditions and design specifications required for the model solution. The detailed description of the model to the case of the column Petlyuk presented in the previous work (Matla-González et al., 2013).

ISSN-On line: 2410-4191

The same can be applied to the CPD model, considering the decrease in size of the intermediate stages (sections 2 and 4) column, which are smaller than the sections 1 and 3, as shown in Figure 1b.

| Parameters | Value |
|---|---|
| Number of components | 3 |
| Return the liquid fraction (β) | 0.322 |
| Return the liquid fraction (α) | 0.631 |
| **Prefactionator (SEC-2)** | |
| Number of stages | 24 |
| Feeding step | 13 |
| Feed flow kmol / s | 1 |
| Diameter, m | 5.63 |
| **Main column** | |
| Number Plates | 44 |
| Liquid feed step | 12 |
| Stage steam feed | 37 |
| Output stage sidestream | 25 |
| Diameter SEC 1 and 3 m | 7.23 |
| Diameter SEC 4, m | 4.53 |
| Reflux ratio, kmol / s | 0.6672 |
| Bottom pressure, kPa | 67.89 |
| Pressure in the dome, kPa | 37.49 |
| Heat input to the reboiler, 106 | 127.24 |
| Stage efficiency,% | 100 |

**Table 1** Parameters of the column

## Considerations in the design of the control

This paper considers the temperature of step 1 (T1) as the controlled variable, and the heat rate (QR) as the manipulated variable. (Ts) Is the temperature of any stage of the section corresponding to section 1 of Figure 1b exhaustion. Assume that Ts is measured without delay and temperature of step 1 (T1) is measured with θ> 0 delay, so T1 and Ts are the primary and secondary measuring respectively the temperature-cascade control temperature.

For control design, we consider input-output models of first order plus delay, calculated from the response to a step change in the rate of heat:

$$\frac{T_1(s)}{QR(s)} = G_{QRT_1}(s) = \frac{K_{QRT_1}}{\tau_{QRT_1}s+1}\exp(-\theta_{QRT_1}s) \quad (1)$$

$$\frac{T_s(s)}{QR(s)} = G_{QRT_s}(s) = \frac{K_{QRT_s}}{\tau_{QRT_1}s+1} \quad (2)$$

where s = d / dt is the Laplace variable, K is the gain, τ is the time constant and θ> 0 is the delay due to the measurements and internal transport.

## Cascade control design

This section backstepping approach to design cascade controller temperature-temperature applies (see Figure 2) in order to counteract the non-linearities. This is accomplished through the use of virtual or passive inputs. Once the design is applied to a stage, this is recursive with the other steps until the actual control input. The cascade control structure is composed of two controllers with feedback where the output of the primary control or master changes the reference point of the slave or control. The output of the secondary control directly affects the final control action. The primary controller is governed by temperature measurement in stage 1 of the column, T1, and calculates the required temperature in the stripping section Ts considered as a virtual controller. In the secondary controller the primary controller provides the reference temperature, Ts, ref, where the manipulated input is the rate of heat, QR.

For the design of the controller is used the method steps tuned Internal Model Control (Skogestad, 2003). For a PI controller, these parameters are the gain Kc controller, and integral time constant τI. These tuning steps are relatively simple analytical rules used to calculate the parameters of the controller in accordance with the following equations:

ISSN-On line: 2410-4191

$$K_c = \frac{1}{K}\frac{\tau_1}{2\theta} \qquad y \qquad \tau_I = \min(\tau_1, 8\theta) \tag{3}$$

Where K, $\tau_I$ and $\theta$ are the process gain, time constant and downtime respectively, obtained in the characterization of the dynamic behavior.

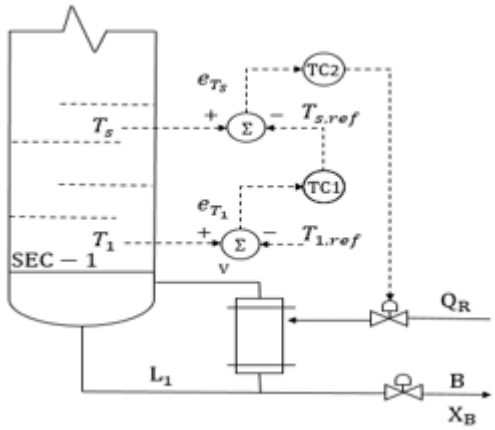


**Figure 2** Structure of backstepping control the stripping section

## Design of the primary controller

The function of the primary loop is to regulate the temperature of step 1, T1, through manipulation of the temperature of the stripping section Ts. For the model input (Ts) -output (T1) combining Eqs. 1 and 2 thus have:

$$G_{T_s,T_1}(s) = \frac{G_{QR,T_1}(s)}{G_{QR,T_s}(s)} = K_{T_s,T_1}\left(\frac{\tau_{QR,T_s}s+1}{\tau_{QR,T_1}s+1}\right)\exp\left(-\theta_{T_s,T_1}s\right) \tag{4}$$

Where $T_{Ts,T1} = K_{QRT1}/ K_{QRTS}$. For close to steady state conditions:

$$G_{T_s,T_1}(s) \approx K_{T_s,T_1}\exp\left(-\theta_{T_s,T_1}s\right) \tag{5}$$

$T_{s,ref}$ is taken instead of the deviation temperature Ts, so that the model for calculating the primary controller is:

$$G_{Tsref,T_1}(s) \approx K_{T_{sref},T_1}\exp\left(-\theta_{T_{sref},T_1}s\right) \tag{6}$$

From Eq. 6 shows the tuning parameters for the primary controller which is kind Proportional-Integral (PI) and operates under the expression described are calculated in Eq. 7

$$T_{s,ref} = T_{s,nom} + K_c\left(\left(T_{1,ref} - T_1(t)\right) + \frac{1}{\tau_I}\int_0^t\left(T_{1,ref} - T_1(t)\right)dt\right) \tag{7}$$

Where $T_{1,ref} - T_1(t) = e_{T1}$ is the error of temperature on dish 1 (bottom).

## Design of the secondary controller

Once built the primary to regulate the bottom temperature by manipulating the trajectory $T_{s,ref}$ plate measured temperature, the controller design objective is to obtain a secondary controller driver manipulates the heat rate so that the temperature fit the set-point variation in the time $T_{s,ref}$ provided by the primary controller. The controller design is based on Eq. 2. The corresponding PI controller is given by Eq. 8, wherein the error calculated by the temperature difference described in Eq. 9

$$QR = \overline{QR}_{nom} + K_c\left(e_{T_s} + \frac{1}{\tau_I}\int_0^t e_{T_s}\,dt\right) \tag{8}$$

$$e_{T_s} = T_{s,ref} - T(t) \tag{9}$$

## Integral Performance Criterions

To evaluate the performance of the proposed control structure is introduced to the system a disturbance in the feed composition in order to observe the response of the controller in the temperature control selected plate SEC-1 which indirectly controls the compositions of the final products.

ISSN-On line: 2410-4191

The dynamic behavior of the error control system is commonly used as a design criterion for tuning PI controllers. The criteria used in this study to measure the performance of the controller was integral absolute error criterion IAE and thus the absolute error of temperature (IAET) and composition (IAEC) (Eq. 10 is obtained and 11).

$$\text{IAET} = \int_0^t [T_{1,\text{ref}} - T_1(t)]dt = \int_0^t e_{T_1}\, dt \quad (10)$$

$$\text{IAEC} = \int_0^t [0.99 - X_B(t)]dt = \int_0^t e_{X_B}\, dt \quad (11)$$

**Results**

In this section the results of the effect of the location of the secondary controller of temperature on the performance of the temperature control back of a CPD and regulating the composition of the bottom product are presented. And parameters characterizing the dynamic behavior of the dividing wall column by a step change in the rate of heat are present, the effect thereof on the temperature of the dishes and on the composition of o-xylene was evaluated. In addition the effect of the location of the temperature measurement on the ability of regulating a cascade control structure in the presence of disturbances in the feed composition is studied.

The step changes ± 1% in heat rate (QR) transfer functions presented in equation (12) were obtained - (19).

$$\frac{T_1}{QR} = G_{T_1,QR}(s) = \frac{(1.19413)e^{0.17711s}}{3.55441s+1} \quad (12)$$

$$\frac{T_2}{QR} = G_{T_2,QR}(s) = \frac{(2.16622)e^{0.14963s}}{3.56565s+1} \quad (13)$$

$$\frac{T_3}{QR} = G_{T_3,QR}(s) = \frac{(3.56539)e^{0.11713s}}{3.5619s+1} \quad (14)$$

$$\frac{T_4}{QR} = G_{T_4,QR}(s) = \frac{(5.29313)e^{0.07963s}}{3.66313s+1} \quad (15)$$

$$\frac{T_5}{QR} = G_{T_5,QR}(s) = \frac{(6.89026)e^{0.04214s}}{3.80186s+1} \quad (16)$$

$$\frac{T_7}{QR} = G_{T_7,QR}(s) = \frac{(7.53903)e^{0.4308s}}{4.3080s+1} \quad (17)$$

$$\frac{T_8}{QR} = G_{T_8,QR}(s) = \frac{(6.30117)e^{0.45667s}}{4.56672s+1} \quad (18)$$

$$\frac{T_9}{QR} = G_{T_9,QR}(s) = \frac{(4.57376)e^{0.47617s}}{4.76171s+1} \quad (19)$$

When designing the seven control loops that regulate the temperature of the dishes, according to the procedure described in Section 4 parameters that characterize it obtained. The results of this characterization are shown in Table 2.

In Table 3 the three disturbances introduced to the system and consisted of changing the feed composition to analyze the behavior of each of the control structures shown in closed loop.

In Table 4 the results of the integral of absolute error of temperature (IAET) and composition (CDAI) are shown, along with the values of settling times each controller. Table shows that the ECC ECC T1-T2 and T1-T3 were the presetaron better performance, however, the settling time is greater in these two structures, diminishing as the secondary controller is located at higher stages.

In Figure 3 the response of the three structures having the best performance in the temperature control plate 1, it is observed that despite the disruption the composition is maintained above 99% purity is shown.

ISSN-On line: 2410-4191

| Cascade control structure | Primary controller | |
|---|---|---|
| | $K_c$(°F/(Btu/h)$^{-1}$) | τI(h) |
| $T_1$-$T_2$ | 0.55125 | 2.66861 |
| $T_1$-$T_3$ | 0.33492 | 1.06707 |
| $T_1$-$T_4$ | 0.33157 | 0.53353 |
| $T_1$-$T_5$ | 0.32487 | 0.44817 |
| $T_1$-$T_7$ | 0.32153 | 0.40546 |
| $T_1$-$T_8$ | 0.31818 | 0.37348 |
| $T_1$-$T_9$ | 0.30478 | 0.41082 |
| | Secondary controller | |
| | $K_c$(°F/(Btu/h)$^{-1}$) | τI(h) |
| $T_1$-$T_2$ | 5.50011 | 1.19708 |
| $T_1$-$T_3$ | 4.26438 | 0.93708 |
| $T_1$-$T_4$ | 3.83795 | 0.91833 |
| $T_1$-$T_5$ | 2.98507 | 0.89866 |
| $T_1$-$T_7$ | 3.71001 | 0.89584 |
| $T_1$-$T_8$ | 4.05117 | 0.81525 |
| $T_1$-$T_9$ | 3.28358 | 0.89491 |

**Table 2** Parameters of the cascade controller

| | P 1 | P 2 | P 3 |
|---|---|---|---|
| Time, h | 20 | 60 | 100 |
| composition% mol | 30/35/35 | 30/30/40 | 35/30/35 |

**Table 3** Disturbances in the system for each cascade control structure

| Cascade control | IAET | IAEC | Settling Time (hr) |
|---|---|---|---|
| ECC $T_1 - T_2$ | 2.212 | 0.17667 | 114.323 |
| ECC $T_1 - T_3$ | 3.162 | 0.10776 | 111.542 |
| ECC $T_1 - T_4$ | 3.772 | 0.12599 | 89.023 |
| ECC $T_1 - T_5$ | 5.925 | 0.16901 | 93.884 |
| ECC $T_1 - T_7$ | 10.47 | 0.23618 | 93.646 |
| ECC $T_1 - T_8$ | 10.48 | 0.26196 | 79.817 |
| ECC $T_1 - T_9$ | 11.71 | 0.27630 | 70.374 |

**Table 4** Comprehensive error and settling time

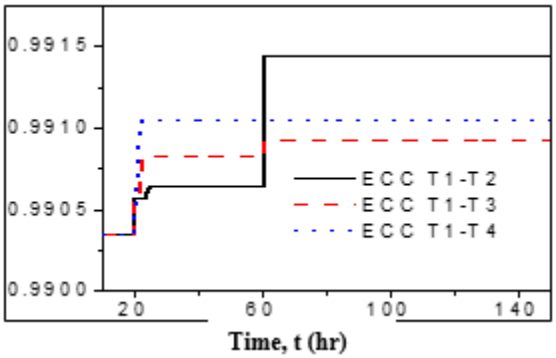


**Figure 3** Performance of the composition of o-xylene to disturbances in the feed composition

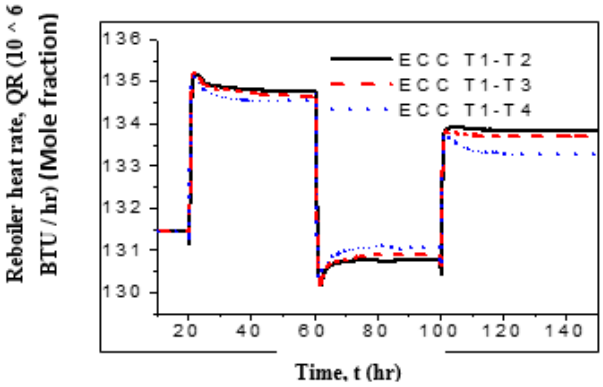


**Figure 4** Response of heat rate to disturbances in the feed composition

In Figure 4 the response of the rate of heat showing the response to reach the steady state occurs, this agrees with the results presented in Table 4, and that the more rapid the rate response time heat settling the temperature of step 1 decrease.

In Figures 5 and 6 the temperature response on the plate 1 of the structures of ECC T1-T2 and ECC T1-T3 control performed better shown, therein it is seen that by introducing our controller proposed in the presence of disturbances, you come to regulate the temperature of the plate 1 by deleting mistakes and reaching the setpoint again. It is also noted that the oscillations decrease when the secondary controller is positioned in upper stages of the stripping section.

ISSN-On line: 2410-4191

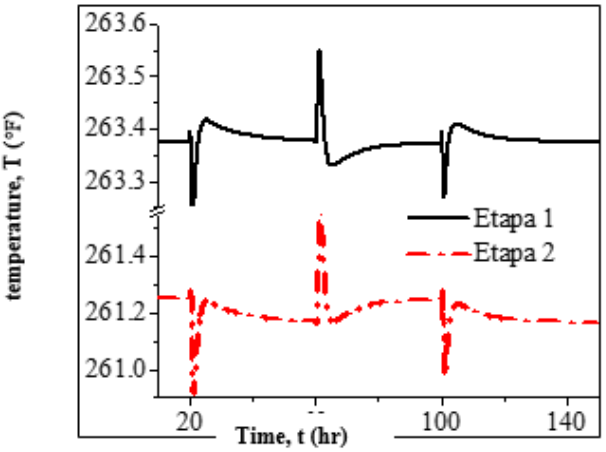


**Figure 5** Response ECC temperature T1-T2

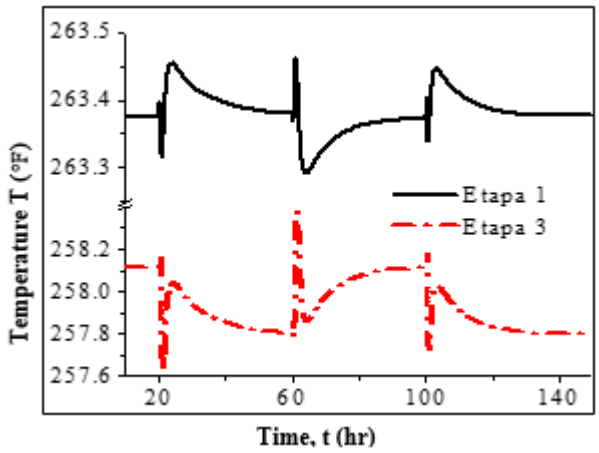


**Figure 6** Response of the temperature of the ECC T1-T3

## Conclusions

Using the Backstepping principle in cascade, which was taken as reference temperature of step 1 (background) corresponding to the primary controller and selecting different than the latter (step 2, 3, 4, 5, 7, 8, 9) stages wherein the secondary controllers for measuring corresponding temperatures, as an indirect measure of the composition regulated by the rate of heat was observed were located that its location has a significant effect in controlling the composition of o-xylene. The use of these controllers in different stages of the grinding part allows to keep the composition of o-xylene above 99.0% purity, from disruption in the feed composition.

From the results it can be seen that the performance will improve as the secondary controller is close to Stage 1 where it aims to keep its temperature setpoint, however, the settling time is greater. This drawback can be reached to improve with the help of a controller designed under the same backstepping approach in the rectifying section, reaching steady state and getting shorter settlement.

## References

Abdul Mutalib M. I., Smith R., (1998). Operation and control of dividing wall columnas part 1: degree of freedom and dynamic simulation. Transaction of the Institution Chemical Engineers 76, part A, 308-318.

Abdul Mutalib M. I., Zeglam A. O., Smith R., (1998). Operation and control of dividing wall columns part 2: simulation and pilot plant studies using temperature control. Transaction of the Institution Chemical Engineers 76, part A, 319-334.

Álvarez-Ramírez J., Monroy-Loperena R., Álvarez J., (2002). Backstepping Design of Composition Cascade Control for Distillation Columns. AIChE, J. 48 (8), 1705-1718.

Castellanos-Sahagún y Álvarez J., (2013). Temperature-Temperature cascade control of binary batch distillation columns. 17-19 Julio. Zürich, Switzerland: European Control Conference.

Kaibel, G. (2002). Process synthesis and design in industrial practice. European Symposium on Computer Aided Process Engineering 12, 9-22, Ed. Elsevier, Holanda.

Ling H., Luyben W. L., (2010). Temperature control of the BTX divided- wall column. Industrial and Engineering Chemistry Research 49 (1), 189-203.

ISSN-On line: 2410-4191

Luan S., Huang K., Wang Y., Wu Ning., (2013). Operation of dividing wall columns.1. A simplified temperature difference control scheme. Industrial and Engineering Chemistry Research (52), 2642-2660.

Luyben W. L., (1969). Feedback control of distillation columns by double differential temperature control. Ind. Eng. Chem. Fundam. 8 (4), 739.

Matla-González D., Urrea-García G., Alvarez-Ramirez J., Bolaños-Reynoso E., Luna-Solano G., (2013). Simulation and control based on temperature measurements for Petlyuk distillation columns. Asia-Pacific Journal of Chemical Engineering 8(6), 880-894.

Medina-Rodríguez L., Urrea-García G., Bolaños-Reynoso E., Pliego-Bravo Y., Efecto de la localización del control de temperatura sobre el destilado en una CPD. Revista del Coloquio de Investigacion Multidisciplinaria 2015, aceptado.

Shin, J., Seo, H., Han, M., Park, S., (2000). A nonlinear profile observer using tray temperatures for high-purity binary distillation columns. Chem. Eng. Sci. 55, 807.

Schultz, M.A., Stewart, D.G., Harris, J.M., Rosenblum, S.P., Shakur, M. S., O'Brien, D., (2002). Reduce Costs with Dividing-Wall Columns. CEP Mayo 2002, www.cepmagazine.org, 64–71.

Serra M., Perrier M., Espuña A., Puigjaner L., (2003). Controllability of different multicomponent distillation Arrangements. Industrial and Engineering Chemistry Research 42, 1773 - 1782.

Skogestad S., (2003). Simple analytic rules for model reduction and PID controller tuning. Journal process control 13, 291-309.

Skogestad S. y Wolff E. A., (1996). Temperature cascade control of distillation. Industrial and Engineering Chemistry Research 35, 475-484.

Rodríguez Hernández, M., Chinea-Herranz, J. A., (2012). Decentralized control and identified-model predictive control of divided wall columns. Journal of Process Control 22 (9), 1582–1592.

ISSN-On line: 2410-4191

Article ECORFAN Journal
OPTICAL June 2015 Vol.2 No.2 101-108

# Portable system for capturing images of the sclera

ROJAS, Carlos*†, ROJAS, Rafael, BAUTISTA, Jorge y TRUJILLO, Valentín

Received January 8, 2014; Accepted June 12, 2015

**Abstract**

For many years in México and the world there is the tendency to improve the health of people, with emphasis on prevention and early detection, one of the most common examples is detection of breast cancer, if it is detected early it is curable. This paper proposes a system for digital image capturing, principally for the detection of the sclera (the white part of the eye), because not are databases available for sclera analysis, only for iris or pupil. The device must be of moderate cost and small size to perform a self-examination in a habitual place for people, can be their home, and were used recycled and low cost materials. It should be noted that the main purpose it is to capture images as uniform as possible, and thereby in the subsequent works, the detection of the sclera is less complicated.

**Diagnosis, eye, image, sclera**

**Citation:** ROJAS, Carlos, ROJAS, Rafael, BAUTISTA, Jorge y TRUJILLO, Valentín. Portable system for capturing images of the sclera. ECORFAN Journal-Bolivia 2015, 2-2: 101-108

* Correspondence to Author (email: carojash@uaemex.mx)
† Researcher contributing first author.

## Introduction

There is a significant amount of systemic diseases, ie affecting various organs of the body, as one of the first symptoms an affectation, color change or deformity of the eyes, primarily in its outer layers, such as the cornea and / or sclera (College of Medicine at Chicago, University of Illinois, 2015) (Zarranz Ventura, De Nova, & Moreno-Montañés, 2008).

Among the most important in terms of number of people with symptoms are: Diabetes mellitus, hepatitis (yellow skin and sclera), hyperbilirubinemia (yellow skin and sclera), osteogenesis imperfecta (blue sclera), acquired immunodeficiency syndrome (AIDS), Arthritis rheumatoid, hypertension and multiple sclerosis.

According to data from the National Health Information System (Ministry of Health of the State of Morelos, 2015) (National Health Information System, 2015), in Mexico more than 75 thousand people die from diabetes mellitus and complications, more than 28,000 from liver disease, more than 15 thousand hypertensive diseases, as well as nearly 5000 HIV / AIDS.

So a periodic review of eyes would help in early detection of damages and therefore a diagnosis and treatment.

This involves performing eye exams periodically, however, for most people is not affordable because the spaces where are these teams are central locations, so make a weekly, daily review or several times a day It is difficult due to the time and cost of transport. Added to this the necessary equipment to obtain the images are often expensive, plus they all are imported. Also to be considered are made primarily to take pictures of the pupil or retina; Three examples are shown in Table 1.

| Equipment | Price (USD) |
|---|---|
| Retinal Camera Kowa nonmyd 7 | $7,999 |
| Scope Horus DEC 100 | $6,000 |
| No mydriatic retinal camera | $4,000 |

**Table 1** Equipment for acquiring images of eyes

From the above revisions and regular eye exams with a team of moderate cost (about $ 600 USD, including computer equipment storage) would help detect systemic diseases; it should be noted that the team is a support tool for the specialist, and does not replace regular reviews recommended.

This paper begins with a brief explanation of the anatomy of the human eye, following the proposed system and conclusions

## Anatomy of the human eye.

Vision is the sense of human beings that allows us to get a lot of information about objects and events around us, it is the dominant sense, so knowing their anatomy is important for the current project, in Figure 1 (human eye and its visible parts, 2014) an image of the human eye as we see in the "daily life" with their respective parties, of which the system will focus on the images, also called the sclera sclera shown.

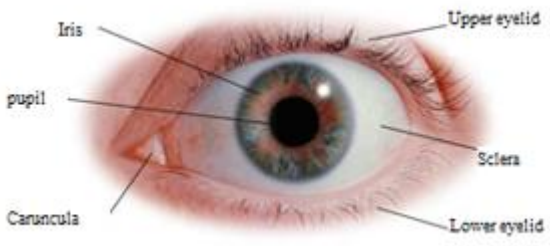


**Figure 1** Human eye and visible parts

ISSN-On line: 2410-4191

**Sclera**

Sclera "is white. It is composed mainly of collagen tissue which gives it extraordinary strength and few blood vessels allowing the white color of the collagen fibers "(Faculty of Medicine, Catholic University of Chile, 2014).

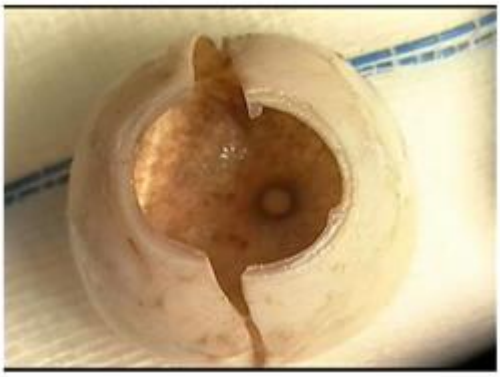

**Figure 2** Sclera [7]

In Figure 2, which was obtained from (González del Valle, Alvarez Portela, Lara Medina Sanchez Celis, Barrajón & Rodriguez, 2012), the sclera after being extracted, showing their shape and color is displayed, it appears that is completely white and clear, so that a change in coloration indicate a disorder itself, which is rare, or a disease of some other organ of the body that is manifested in the sclera.

Note that in Figure 1 only you can identify a part of the sclera, so it is necessary to capture more than one image to obtain a larger surface, for it is proposed to capture at least five images with different eye movements for improve the analysis of the sclera.

**Proposed system**

**The system consists of 3 main parts**

Image acquisition: two commercial web cameras inexpensive one for each eye are used, we underline that the system must be affordable so it can be acquired by people of all social strata, and the characteristics are shown in Table 2.

Although the limited camera features are sufficient for the desired images, such databases are images of eyes among which UBIRIS (Proença & Alexander, 2005) used in the iris detection and its applications in its first version the resolution is 800 x 600 pixels, the same resolution as the cameras used.

| Web Cam Perfect Choice | |
|---|---|
| sensor | CMOS SVGA, 480 Kpixels |
| sampling | 30 fps |
| resolution | 800 x 600 pixels (up to 8MP interpolated by software) |
| feeding | 5 Vcc , 150 mA |
| dimensions | 5.4 x 5.4 x 8 cms |

**Table 2** Characteristics of the webcam

Lighting: In the acquisition of the images is necessary that the lighting is uniform, so the preprocessing and processing will be reduced if these are used to detect the sclera, iris or some other part of the eye, and if there is a change in shape or color.

As the device is said to be small in size, so has chosen to use LED surface mount that emit white light, 3 (LED surface mount 0805W2C-KHC-B, 2015), with the characteristics obtained from (Data Sheet SMD LED 0805W2C-KHC-A, 2015) that are shown in Table 3.

ISSN-On line: 2410-4191

**Figure 3** LED surface mount 0805W2C-KHC-B [9]

LEDs are placed around the lens of the webcam, which was previously separated from her deck, were tested with 2 and 4 LED, in both cases the results were satisfactory as shown in Figure 4 and Figure 5.

Importantly, the intensity of the lighting should be regulated to avoid any damage to the eyes, as the camera and the LED is confined in a cardboard tube that besides avoiding there external lighting, not allowing light to go out and improve the image; the regulation is performed by a microcontroller Arduino Mini by pulse width modulation, PWM for its acronym in English.

| SMD LED 0805W2C-KHC-A | |
|---|---|
| material | AlGaN |
| Luminous intensity | 200 – 300 mcd |
| voltage | 2.9 – 3.5 V |
| current | 30 mA |
| Viewing angle | 120º |
| High | 1.1 mm |
| Width | 1.25 mm |
| Long | 2.0 mm |

**Table 3** Characteristics of LED [10]

Capture and storage: To preserve the images, the cameras are connected via USBconnectors to a personal computer. A DellInspiron 3647 computer was used, with the characteristics described in Table 4 in this case.

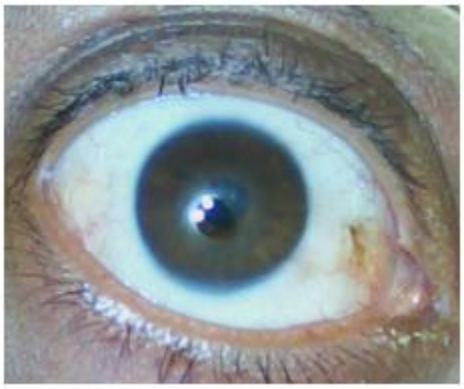

**Figure 4** Image taken with 2 LED

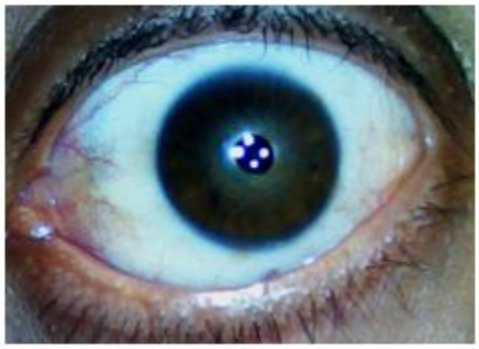

**Figure 5** Image taken with 4 LED

The operating system used is Windows 8 by the manufacturer, the software for the acquisition and display of images is Mathworks Matlab R2012b installed.

ISSN-On line: 2410-4191

| Dell Inspiron 3647 | |
|---|---|
| processor | Intel® Core™ i5-4460S |
| RAM | Memory 8GB Dual Channel DDR3 at 1600MHz |
| Hard disk | SATA de 1TB 7200 RPM |
| Optical drive | CD/DVD +/- RW 16x |
| video card | Intel HD integrated graphics |
| Display | Dell 20 inches |

**Table 4** Characteristics of the personal computer

With the same software interface was made to show both chambers and be able to take the two pictures with the touch of a button, which is shown in Figure 6.

**Figure 6** Interface conducted in Matlab for two cameras

The code in Matlab to display both video streams from the cameras is as follows:

```
% Create video objects with a resolution of 800x600 pixels
camara_izq = videoinput ('WinVideo', 1 'RGB24_800x600');
videoinput camera = ('WinVideo', 2, 'RGB24_800x600');
figure ('Number Title', 'of', 'Name', 'Chambers');
% Subwindow left chamber
previo_izq = subplot (1,2,1);
axes (previo_izq);
tam_izq = image (zeros (800,600));
preview (camara_izq, tam_izq);
% Right subwindow camera
previo_der = subplot (1,2,2);
axes (previo_der);
tam_der = image (zeros (640.480));
preview (camara_der, tam_der);
```

Once both sequences are displayed with the "Taking Pictures" from the bottom of the interface, photographs are taken of the eye, the code shown below:

```
uicontrol ('String', 'Take Photo', ... 'Callback', 'figure (1), frame1 = getsnapshot (camara_der) figure, imshow (frame1) 4figure (2), frame2 = getsnapshot (camara_izq); figure, imshow (frame2); '...' Units', 'normalized', ... 'Position', [0.60 0.15 0 .07])
```

In most cases, preliminary tests are with the pupil facing forward so, it is proposed four photographs are taken with the pupil looking around, inside and outside as shown in Figure 7

**Figure 7** Pupil the outside and inside

Furthermore two images with the pupil looking up and down as shown in Figure 8.

**Figure 8** Pupil up and down

ISSN-On line: 2410-4191

With the capture of the 5 images could observe a greater surface area of the sclera, making it possible to detect any changes in it would be very difficult with images from other databases, as these are only planned for iris detection (front view).

Once the images are captured, the names of the files to be stored is important to follow a pattern for the date, time and the "place" to where the pupil is oriented so that the file name is relatively short and is have as much information as possible without opening or display its properties, a format with the following options are proposed:

Eye: left (left), der (right)
Date: DDMMYY (day, month, year)
Time: hhmm (hours, minutes)
Pupil: CEN (center), int (internal), ext (external), arr (above), aba (below)
An example of the name of a stored image is:
der_121214_1000_cen.jpg

Information that can be deduced from the file name is: right eye photo taken on December 12, 2014 at 10:00 hours with the pupil center. This is important, as discussed 5 photos are taken by each eye, to have 10 images per acquisition, since being a device support in the diagnosis of changes in the sclera is necessary to perform one or more catches on different days and hours for a more reliable study.

Because one of the problems, as mentioned above, is the cost and time of transfer to visit the specialist; It arises generate a database as a medical record for each person.

The necessary basic fields are the name, age and sex, including the set of eye images taken which are already in the format mentioned, an example of the diagram to the database shown in Figure 9.

However this model may be appropriate based on user requirements or specialist.

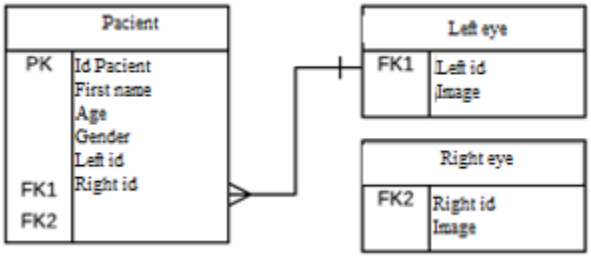


**Figure 9** Diagram for the database

## Results

The first tests and prototypes were developed with inexpensive materials such as cardboard rolls, silicone, cheap web cameras, lenses for welding to name a few.

When the improvement of image capture is achieved, the CAD design software is performed to suit the anthropometric measures of most people and the final prototype through a 3D printer.

Furthermore it has the support of the student community of the Autonomous University of the State of Mexico Zumpango CU, to begin forming a database of sclera. This is to innovate in an area which does not have such information.

## Conclusions

A prototype of the system with low cost materials and small dimensions, with encouraging results is done because the captured images have a uniform illumination with an appropriate resolution; storage is also done automatically on a personal computer by pressing a button on the graphical interface.

ISSN-On line: 2410-4191

Captured images of the sclera preprocessing, processing or detection of the sclera have minor complications, because the images will be homogeneous, and the analysis and diagnosis of diseases may be more reliable.
It considered for future work the cameras are connected to the microcontroller and therefore the images are stored in the cache memory, whether external or internal, also taking advantage of the characteristics of Arduino could be sent wirelessly to a computer or smartphone for processing without a cable analysis.

By having a sufficient amount of database images with enhanced features, similar to those that exist in the study of the pupil or iris compile, and software for the processing, analysis and diagnosis of diseases will be scheduled.

It also intends in the future to provide the database obtained to facilitate investigations associated with the sclera.

**References**

College of Medicine at Chicago, University of Illinois. (2015). The Eye in Systemic Disease. Recuperado el 12 de mayo de 2015, de The Illinois Eye and Ear Infirmary: http://chicago.medicine. uic.edu/cms/One.aspx?portalId=506244&pageId=15427346

Facultad de Medicina, Pontificia Universidad Católica de Chile. (2014). Información básica de Anatomía ocular. Recuperado el 20 de mayo de 2015, de http://escuela.med.puc.cl/paginas/Cursos/quinto/Especialidades/Oftalmologia/pdf/AnatomiaOcular2011.pdf.

González del Valle, F., Álvarez Portela, M., Lara Medina, J., Celis Sánchez, J., & Barrajón Rodríguez, A. (2012). Técnica de extracción de esclera donante mediante extrusión del globo ocular. Archivos de la Sociedad Española de Oftalmología , 87 (9), 294-296.

Hoja de especificaciones SMD LED 0805W2C-KHC-A. (2015). Recuperado el 18 de julio de 2015, de www.beeled.ru/images/3001/0805W2C-KHB-A.pdf

LED de montaje superficial 0805W2C-KHC-B. (2015). Recuperado el 16 de julio de 2015, de A-electronics, Robótica y electrónica: http://a-electronics.com.mx/img/p/8/9/9/899-thickbox_default.jpg

Ojo humano y sus partes visibles. (2014). Recuperado el 20 de junio de 2015, de Nebraska Medice: http://www.nebraskamed.com/app_files/images/staywell/126294.jpg

Proença, H., & Alexandre, L. (2005). UBIRIS: A noisy iris image database. 13th International Conference on Image Analysis and Processing - ICIAP 2005. LNCS 3617, págs. 970-977. Cagliari, Italy: Springer.

Secretaría de Salud del Estado de Morelos. (2015). Datos estadísticos sobre principales problemas de Salud Pública . Recuperado el 18 de mayo de 2015, de Servicios de salud de Morelos: http://www.ssm.gob.mx/portal/index.php/2-uncategorised/11-salud-publica

Sistema Nacional de Información en Salud. (2015). Principales causas de mortalidad general 2000 - 2008. Recuperado el 18 de mayo de 2015, de http://sinais.salud.gob.mx/descargas/xls/m_005.xls

ISSN-On line: 2410-4191

Zarranz Ventura, J., De Nova, E., & Moreno-Montañés, J. (2008). Corneal manifestations in systemic diseases. An Sist Sanit Navar , 31 (3), 155-70.

ISSN-On line: 2410-4191

Article ECORFAN Journal
RESOURCES June 2015 Vol.2 No.2 109-117

# The method of small perturbations to Calculate Stiffness and damping in a Short Chumacera

RAMIREZ, Ignacio*†`, CANO, Alexis` and ANTONIO, Alberto

*`Instituto Tecnológico de Pachuca. División de Estudios de Posgrado e Investigación. Carretera México-Pachuca Km 87.5, Col. Venta Prieta, Pachuca de Soto, Hidalgo. MEXICO*
*``Instituto de Electrónica y Computación, Universidad Tecnológica de la Mixteca. Huajuapan de León, Oaxaca, MEXICO, CP 69000*

Received January 8, 2014; Accepted June 12, 2015

## Abstract

In this paper, an alternative method to characterize a hydrodynamic bearing is presented. Based on the Reynolds' general lubrication equation, a perturbation is made on the center of the journal in order to partial pressures, so that be able to manage them to determine both the stiffness and damping dynamic coefficients. It is done the calculation for a classical case and it is generalized to situations that involve external excitations. The dynamic coefficients are gotten in an analytical way and they are plotted as a function of the balance eccentricity. The methodology presented in this document is of great value because it can be adapted for complex cases to get quite acceptable numerical solutions.

**Reynolds, Rotordynamics, Journal Bearing.**

**Citation:** RAMIREZ, Ignacio, CANO, Alexis and ANTONIO, Alberto. The method of small perturbations to Calculate Stiffness and damping in a Short Chumacera. ECORFAN Journal-Bolivia 2015, 2-2: 109-117

* Correspondence to Author (email: tijonov@hotmail.com)
† Researcher contributing first author.

## Introduction

The equations of motion of a system-rotor bearings contain coefficients corresponding to the lubricant film. These parameters change with the position having the shaft relative to the bearing center and the rotation speed. That's why the dynamic behavior is always heavily influenced by the values they can take these coefficients. It is in the literature as the operation speed increases, one of the stiffness coefficients can take negative values depending on its magnitude and the system could instability [1].

To study the behavior of the fluid in the hydrodynamic bearings Reynolds equation is used, which is a simplification of the Navier-Stokes equations for Newtonian fluids type. Reynolds equation relates the fluid pressure in the bearing with axial and circumferential coordinates, so it is possible to obtain the pressure field. It is not possible to analytically solve the Reynolds equation, but approaches are available depending on the length / diameter of the bearing (L / D) ratio. However, it is possible to determine the dynamic condition of the lubricant film taking the linear behavior of the pressure field and forces it along. Disturbing the equilibrium position of the stump to find modifying pressure increases the dynamic properties of the support and highlight the effect of stiffness and damping of the oil film.

## Nomenclature

C: Clear radial bearing
$c_{ij}$: Damping coefficients
$D$: Diameter of the bearing
$e$: Eccentricity
$H$: Thickness o the lubricant film
$h$: Dimensionless film thickness
$k_{ij}$: Stiffness coefficients
$L$: Length of the bearing
$N$: Operating speed
$p$: Pressure of the lubricant film
$S$: Sommerfeld number
$z$: Axial Cartesian coordinate
$\phi$: Angle of attitude.
$\theta$: Circunferential coordinates of bearing
$\varepsilon$: Dimensionless exxentricity, $\varepsilon$=e/C
$\omega$: Operating speed.
$\mu$: Dynamic or Absotlute viscosity.

## Development

The model describing the function of pressure in hydrodynamic bearings is the Reynolds equation; such an equation can be written generally as [2]:

$$\frac{1}{R_1^2}\frac{\partial}{\partial\tilde{\theta}}\left(\frac{H^3}{12\mu}\frac{\partial p}{\partial\tilde{\theta}}\right)+\frac{\partial}{\partial z}\left(\frac{H^3}{12\mu}\frac{\partial p}{\partial z}\right)=\frac{\omega}{2}\frac{\partial H}{\partial\tilde{\theta}}+\frac{\partial H}{\partial t} \tag{1}$$

This equation can be written in dimensionless form using the following parameters: $H = Ch = C[1+\varepsilon\cos(\tilde{\theta}-\phi)]$ (2)

$$z=\frac{L}{2}\bar{z}\ \ , p=\mu N\left(\frac{R_1}{C}\right)^2\bar{p}\ , \qquad \omega = 2\pi N \tag{3}$$

Substituting this in equation (1) is obtained in dimensionless form as:

$$\frac{\partial}{\partial\tilde{\theta}}\left(h^3\frac{\partial\bar{p}}{\partial\tilde{\theta}}\right)+\left(\frac{D}{L}\right)^2\frac{\partial}{\partial\bar{z}}\left(h^3\frac{\partial\bar{p}}{\partial\bar{z}}\right)=12\pi\frac{\partial h}{\partial\tilde{\theta}}+\frac{24\pi}{\omega}\frac{\partial h}{\partial t} \tag{4}$$

With the boundary conditions:

$p=0$ for $z=\pm L/2$ y $\left(\frac{\partial p}{\partial z}\right)=0$ para $z=0$.

Note that: $\tilde{\theta}=\theta+\phi$ , $h=1+\varepsilon\cos(\tilde{\theta}-\phi)$.

In Figure 1 a given rotor (stump in the bearing) illustrated position, the parameters included in Reynolds equation is:

ISSN-On line: 2410-4191

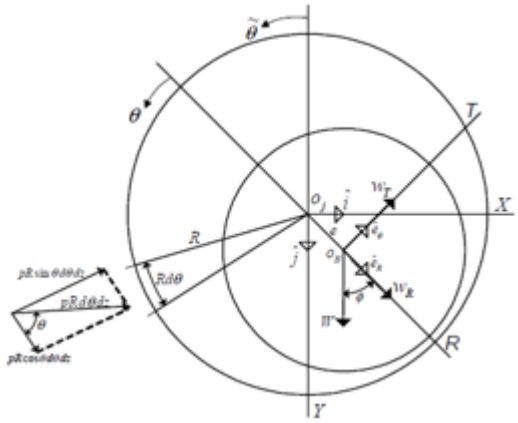

**Figure 1** Instantaneous position of the rotor within the bearing

The proposed methodology is performed by making small perturbations around the equilibrium position. The fact only considering small perturbations is necessary because the equations of motion of rotor-bearings are highly nonlinear system. For example, consider the case of a mass 2M rotor supported by two identical bearings and properly aligned. The equations of motion are [1]:

$$\begin{Bmatrix} M & 0 \\ 0 & M \end{Bmatrix} \frac{\partial^2}{\partial t^2} \begin{Bmatrix} a\cos\phi \\ a\sin\phi \end{Bmatrix} = \begin{Bmatrix} W\cos\phi_t \\ W\sin\phi_t \end{Bmatrix} - \begin{Bmatrix} F_Y \\ F_X \end{Bmatrix} \tag{5}$$

Where $F_X$ y $F_Y$ are reaction forces in the bearings. These equations are highly nonlinear and even when known $W$ and $\phi_t$ as functions of time. The method used to deal with this type of equations is linearized reaction forces of the bearings around its equilibrium position. Figure 2 depicts the effect produced by the load changes on the position of the bearing axis. The zero subscript refers to Figure steady state position and $\Delta x$ , $\Delta y$ indicate the displacements of the shaft about its equilibrium position or small displacements of disturbance. Calculating the change in these small perturbations with respect to time is obtained speeds disturbance $\Delta\dot{x}$ and $\Delta\dot{y}$ [3].

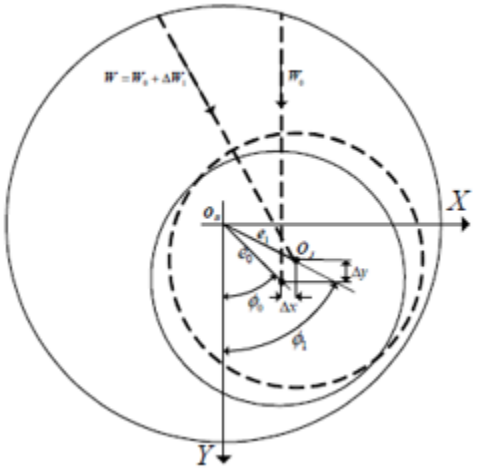

**Figure 2** rotor position change made by disturbances.

The resulting reaction force F = W of Figure 2 has components $F_X$ and $F_Y$. It made Taylor series expansions of the first order of these components is obtained:

$$F_X = (F_X)_0 + \left(\frac{\partial F_X}{\partial x}\right)_0 \Delta x + \left(\frac{\partial F_X}{\partial y}\right)_0 \Delta y + \left(\frac{\partial F_X}{\partial \dot{x}}\right)_0 \Delta\dot{x} + \left(\frac{\partial F_X}{\partial \dot{y}}\right)_0 \Delta\dot{y} \tag{6}$$

$$F_Y = (F_Y)_0 + \left(\frac{\partial F_Y}{\partial x}\right)_0 \Delta x + \left(\frac{\partial F_Y}{\partial y}\right)_0 \Delta y + \left(\frac{\partial F_Y}{\partial \dot{x}}\right)_0 \Delta\dot{x} + \left(\frac{\partial F_Y}{\partial \dot{y}}\right)_0 \Delta\dot{y} \tag{7}$$

The Y-axis direction is chosen such that $(F_X)_0 = 0$. Note that the partial derivatives of the forces with respect to the position and velocity, respectively represent the stiffness and damping in the lubricant film; then you can write:

$$k_{xx} = \left(\frac{\partial F_X}{\partial x}\right)_0 \qquad k_{xy} = \left(\frac{\partial F_X}{\partial y}\right)_0$$

$$k_{yx} = \left(\frac{\partial F_Y}{\partial x}\right)_0 \qquad k_{yy} = \left(\frac{\partial F_Y}{\partial y}\right)_0$$

$$c_{xx} = \left(\frac{\partial F_X}{\partial \dot{x}}\right)_0 \qquad c_{xy} = \left(\frac{\partial F_X}{\partial \dot{y}}\right)_0$$

$$c_{yx} = \left(\frac{\partial F_Y}{\partial \dot{x}}\right)_0 \qquad c_{yy} = \left(\frac{\partial F_Y}{\partial \dot{y}}\right)_0$$

This allows the equations (6) and (7) can be written as:

ISSN-On line: 2410-4191

$$\begin{Bmatrix} F_X \\ F_Y \end{Bmatrix} = \begin{Bmatrix} 0 \\ (F_Y)_0 \end{Bmatrix} + \begin{pmatrix} k_{xx} & k_{xy} \\ k_{yx} & k_{yy} \end{pmatrix} \begin{Bmatrix} \Delta x \\ \Delta y \end{Bmatrix} + \begin{pmatrix} c_{xx} & c_{xy} \\ c_{yx} & c_{yy} \end{pmatrix} \begin{Bmatrix} \Delta \dot{x} \\ \Delta \dot{y} \end{Bmatrix} \tag{8}$$

Therefore, once the motion equations are linearized, they can easily solve the linearized after determining coefficients $k_{ij}$ and $c_{ij}$.

In the Cartesian coordinate system, the forces in the lubricant film are written as [4]:

$$F_X = \int_{-L/2}^{L/2} \int_{\tilde{\theta}_1}^{\tilde{\theta}_2} pR \sin\tilde{\theta}\, d\tilde{\theta}\, dz \tag{9}$$

$$F_Y = \int_{-L/2}^{L/2} \int_{\tilde{\theta}_1}^{\tilde{\theta}_2} pR \cos\tilde{\theta}\, d\tilde{\theta}\, dz \tag{10}$$

In dimensionless form it can be written:

$$\overline{F}_X = \frac{F_X}{\mu NLD(R/C)^2} = \frac{1}{4} \int_{-1}^{1} \int_{\tilde{\theta}_1}^{\tilde{\theta}_2} \overline{p} \sin\tilde{\theta}\, d\tilde{\theta}\, dz \tag{11}$$

$$\overline{F}_Y = \frac{F_Y}{\mu NLD(R/C)^2} = \frac{1}{4} \int_{-1}^{1} \int_{\tilde{\theta}_1}^{\tilde{\theta}_2} \overline{p} \cos\tilde{\theta}\, d\tilde{\theta}\, dz \tag{12}$$

To enter the effect of disturbance, note that in Figure 2 the position of the stump and the steady state position when there is associated a small perturbation. This can be quantified as:

$$\begin{aligned} e_0 \sin\phi_0 + \Delta x &= e \sin\phi \\ e_0 \cos\phi_0 + \Delta y &= e \cos\phi \end{aligned} \tag{13}$$

Substituting the above expressions into equation film thickness (2) and whereas $\varepsilon = e/C$ and $h = H/C$ dimensionless film thickness is obtained.

$$h = h_0 + \Delta X \sin\tilde{\theta} + \Delta Y \cos\tilde{\theta} \tag{14}$$

Where:

$h_0 = 1 + \varepsilon_0 \cos(\tilde{\theta} - \phi_0)$, $X = x/C$ y $Y = y/C$.

It derives equation (14) with respect to time yields:

$$\frac{dh}{dt} = \omega(\Delta X' \sin\tilde{\theta} + \Delta Y' \cos\tilde{\theta}) \tag{15}$$

Note that $\tau = \omega t$ and raw indicate the change from $\tau$. Thus, to calculate the equilibrium conditions and the coefficients of the lubricant film, it is necessary to solve the Reynolds equation (4), subject to the boundary conditions given and disturbing with (14) and (15).

**General methodology**

Now the description of the methodology used in solving the Reynolds equation is performed by disturbances. Since the analysis is linear, the pressure in the oil film can be expressed as:

$$p = (p)_0 + \left(\frac{\partial p}{\partial x}\right)_0 \Delta x + \left(\frac{\partial p}{\partial y}\right)_0 \Delta y + \left(\frac{\partial p}{\partial \dot{x}}\right)_0 \Delta \dot{x} + \left(\frac{\partial p}{\partial \dot{y}}\right)_0 \Delta \dot{y} \tag{16}$$

Doing:

$$(p)_0 = p_0, \quad \left(\frac{\partial p}{\partial x}\right)_0 = p_x, \quad \left(\frac{\partial p}{\partial y}\right)_0 = p_y, \quad \left(\frac{\partial p}{\partial \dot{x}}\right)_0 = p_{\dot{x}}, \quad \left(\frac{\partial p}{\partial \dot{y}}\right)_0 = p_{\dot{y}}$$

The components of force in the bearings are by integrating the pressure on the bearing area, so we can write:

$$\begin{Bmatrix} F_X \\ F_Y \end{Bmatrix} = \int_z \int_{\tilde{\theta}} (p_0 + p_x \Delta x + p_y \Delta y + p_{\dot{x}} \Delta \dot{x} + p_{\dot{y}} \Delta \dot{y}) \begin{Bmatrix} \sin\tilde{\theta} \\ \cos\tilde{\theta} \end{Bmatrix} R_1 d\tilde{\theta}\, dz \tag{17}$$

The terms of disturbance $\Delta x$, $\Delta y$, $\Delta \dot{x}$ and $\Delta \dot{y}$ are independent of integration variables, therefore, for (17):

$$\begin{Bmatrix} 0 \\ (F_Y)_0 \end{Bmatrix} = \begin{Bmatrix} \int_z \int_{\tilde{\theta}} p_0 \sin\tilde{\theta}\, R_1 dz d\tilde{\theta} \\ \int_z \int_{\tilde{\theta}} p_0 \cos\tilde{\theta}\, R_1 dz d\tilde{\theta} \end{Bmatrix} \tag{18}$$

ISSN-On line: 2410-4191

$$\begin{Bmatrix} k_{xx} & k_{xy} \\ k_{yx} & k_{yy} \end{Bmatrix} = \begin{Bmatrix} \int_z \int_{\tilde{\theta}} p_x \sin\tilde{\theta} R_1 dz d\tilde{\theta} & \int_z \int_{\tilde{\theta}} p_y \sin\tilde{\theta} R_1 dz d\tilde{\theta} \\ \int_z \int_{\tilde{\theta}} p_x \cos\tilde{\theta} R_1 dz d\tilde{\theta} & \int_z \int_{\tilde{\theta}} p_y \cos\tilde{\theta} R_1 dz d\tilde{\theta} \end{Bmatrix} \tag{19}$$

$$\begin{Bmatrix} c_{xx} & c_{xy} \\ c_{yx} & c_{yy} \end{Bmatrix} = \begin{Bmatrix} \int_z \int_{\tilde{\theta}} p_{\dot{x}} \sin\tilde{\theta} R_1 dz d\tilde{\theta} & \int_z \int_{\tilde{\theta}} p_{\dot{y}} \sin\tilde{\theta} R_1 dz d\tilde{\theta} \\ \int_z \int_{\tilde{\theta}} p_{\dot{x}} \cos\tilde{\theta} R_1 dz d\tilde{\theta} & \int_z \int_{\tilde{\theta}} p_{\dot{y}} \cos\tilde{\theta} R_1 dz d\tilde{\theta} \end{Bmatrix} \tag{20}$$

To determine the coefficients $k_{ij}$ and $c_{ij}$, you need to get disturbances pressure field first. Substituting the equations of disturbed film (14), (15) and (16) in the Reynolds equation (4) yields:

$$\begin{aligned} &\frac{\partial}{\partial\tilde{\theta}}\left[(h_0+\Delta X\sin\tilde{\theta}+\Delta Y\cos\tilde{\theta})^3\frac{\partial}{\partial\tilde{\theta}}(\bar{p}_0+\bar{p}_X\Delta X+\bar{p}_Y\Delta Y+\bar{p}_{X'}\Delta X'+\bar{p}_{Y'}\Delta Y')\right]+ \\ &+\left(\frac{D}{L}\right)^2\frac{\partial}{\partial\bar{z}}\left[(h_0+\Delta X\sin\tilde{\theta}+\Delta Y\cos\tilde{\theta})^3\frac{\partial}{\partial\bar{z}}(\bar{p}_0+\bar{p}_X\Delta X+\bar{p}_Y\Delta Y+\bar{p}_{X'}\Delta X'+\bar{p}_{Y'}\Delta Y')\right] \\ &=12\pi\frac{\partial}{\partial\tilde{\theta}}(h_0+\Delta X\sin\tilde{\theta}+\Delta Y\cos\tilde{\theta})+24\pi(\Delta X'\sin\tilde{\theta}+\Delta Y'\cos\tilde{\theta}) \end{aligned} \tag{21}$$

Developing the term $(h_0+\Delta X\sin\tilde{\theta}+\Delta Y\cos\tilde{\theta})^3$ and removed the higher-order terms, the Reynolds equation is obtained with only first-order terms.

$$\begin{aligned} &\frac{\partial}{\partial\tilde{\theta}}\left[(h_0^3+3h_0^2\sin\tilde{\theta}\Delta X+3h_0^2\cos\tilde{\theta}\Delta Y)\frac{\partial}{\partial\tilde{\theta}}(\bar{p}_0+\bar{p}_X\Delta X+\bar{p}_Y\Delta Y+\bar{p}_{X'}\Delta X'+\bar{p}_{Y'}\Delta Y')\right]+ \\ &+\left(\frac{D}{L}\right)^2\frac{\partial}{\partial\bar{z}}\left[(h_0^3+3h_0^2\sin\tilde{\theta}\Delta X+3h_0^2\cos\tilde{\theta}\Delta Y)\frac{\partial}{\partial\bar{z}}(\bar{p}_0+\bar{p}_X\Delta X+\bar{p}_Y\Delta Y+\bar{p}_{X'}\Delta X'+\bar{p}_{Y'}\Delta Y')\right] \\ &=12\pi\frac{\partial}{\partial\tilde{\theta}}(h_0+\Delta X\sin\tilde{\theta}+\Delta Y\cos\tilde{\theta})+24\pi(\Delta X'\sin\tilde{\theta}+\Delta Y'\cos\tilde{\theta}) \end{aligned} \tag{22}$$

Bringing terms of the order is obtained the following set of equations:

$$\frac{\partial}{\partial\tilde{\theta}}\left(h_0^3\frac{\partial\bar{p}_0}{\partial\tilde{\theta}}\right)+\left(\frac{D}{L}\right)^2\frac{\partial}{\partial\bar{z}}\left(h_0^3\frac{\partial\bar{p}_0}{\partial\bar{z}}\right)=12\pi\frac{\partial h_0}{\partial\tilde{\theta}}$$

$$\begin{aligned} &\frac{\partial}{\partial\tilde{\theta}}\left(h_0^3\frac{\partial\bar{p}_X}{\partial\tilde{\theta}}\right)+\left(\frac{D}{L}\right)^2\frac{\partial}{\partial\bar{z}}\left(h_0^3\frac{\partial\bar{p}_X}{\partial\bar{z}}\right)= \\ &=12\pi\cos\tilde{\theta}-\frac{\partial}{\partial\tilde{\theta}}\left(3h_0^2\sin\tilde{\theta}\frac{\partial p_0}{\partial\tilde{\theta}}\right)-\left(\frac{D}{L}\right)^2\frac{\partial}{\partial\bar{z}}\left(3h_0^2\sin\tilde{\theta}\frac{\partial\bar{p}_0}{\partial\bar{z}}\right) \\ &\frac{\partial}{\partial\tilde{\theta}}\left(h_0^3\frac{\partial\bar{p}_Y}{\partial\tilde{\theta}}\right)+\left(\frac{D}{L}\right)^2\frac{\partial}{\partial\bar{z}}\left(h_0^3\frac{\partial\bar{p}_Y}{\partial\bar{z}}\right)= \\ &=-12\pi\sin\tilde{\theta}-\frac{\partial}{\partial\tilde{\theta}}\left(3h_0^2\cos\tilde{\theta}\frac{\partial p_0}{\partial\tilde{\theta}}\right)-\left(\frac{D}{L}\right)^2\frac{\partial}{\partial\bar{z}}\left(3h_0^2\cos\tilde{\theta}\frac{\partial\bar{p}_0}{\partial\bar{z}}\right) \\ &\frac{\partial}{\partial\tilde{\theta}}\left(h_0^3\frac{\partial\bar{p}_{X'}}{\partial\tilde{\theta}}\right)+\left(\frac{D}{L}\right)^2\frac{\partial}{\partial\bar{z}}\left(h_0^3\frac{\partial\bar{p}_{X'}}{\partial\bar{z}}\right)=24\pi\sin\tilde{\theta} \\ &\frac{\partial}{\partial\tilde{\theta}}\left(h_0^3\frac{\partial\bar{p}_{Y'}}{\partial\tilde{\theta}}\right)+\left(\frac{D}{L}\right)^2\frac{\partial}{\partial\bar{z}}\left(h_0^3\frac{\partial\bar{p}_{Y'}}{\partial\bar{z}}\right)=24\pi\cos\tilde{\theta} \end{aligned} \tag{23}$$

The second and third terms on the right side of the second of the above equations can be written as:

$$\begin{aligned} &\frac{\partial}{\partial\tilde{\theta}}\left(3h_0^2\sin\tilde{\theta}\frac{\partial\bar{p}_0}{\partial\tilde{\theta}}\right)+\left(\frac{D}{L}\right)^2\frac{\partial}{\partial\bar{z}}\left(3h_0^2\sin\tilde{\theta}\frac{\partial p_0}{\partial\bar{z}}\right) \\ &=\frac{\partial}{\partial\tilde{\theta}}\left(3h_0^3\frac{\sin\tilde{\theta}}{h_0}\frac{\partial\bar{p}_0}{\partial\tilde{\theta}}\right)+\left(\frac{D}{L}\right)^2\frac{\partial}{\partial\bar{z}}\left(3h_0^3\frac{\sin\tilde{\theta}}{h_0}\frac{\partial\bar{p}_0}{\partial\bar{z}}\right) \\ &=\frac{3\sin\tilde{\theta}}{h_0}\underbrace{\left[\frac{\partial}{\partial\tilde{\theta}}\left(h_0^3\frac{\partial\bar{p}_0}{\partial\tilde{\theta}}\right)+\left(\frac{D}{L}\right)^2\frac{\partial}{\partial\bar{z}}\left(h_0^3\frac{\partial\bar{p}_0}{\partial\bar{z}}\right)\right]}_{12\pi\frac{\partial h_0}{\partial\tilde{\theta}}}+3h_0^3\frac{\partial\bar{p}_0}{\partial\tilde{\theta}}\frac{\partial}{\partial\tilde{\theta}}\left(\frac{\sin\tilde{\theta}}{h_0}\right) \end{aligned}$$

Therefore:

$$\begin{aligned} &\frac{\partial}{\partial\tilde{\theta}}\left(3h_0^2\sin\tilde{\theta}\frac{\partial\bar{p}_0}{\partial\tilde{\theta}}\right)+\left(\frac{D}{L}\right)^2\frac{\partial}{\partial\bar{z}}\left(3h_0^2\sin\tilde{\theta}\frac{\partial\bar{p}_0}{\partial\bar{z}}\right)= \\ &=12\pi\frac{\partial h_0}{\partial\tilde{\theta}}\left(\frac{3\sin\tilde{\theta}}{h_0}\right)+3h_0^3\frac{\partial\bar{p}_0}{\partial\tilde{\theta}}\frac{\partial}{\partial\tilde{\theta}}\left(\frac{\sin\tilde{\theta}}{h_0}\right) \end{aligned}$$

Equal to the second and third terms on the right side of the third of the preceding equations:

$$\begin{aligned} &\frac{\partial}{\partial\tilde{\theta}}\left(3h_0^2\cos\tilde{\theta}\frac{\partial\bar{p}_0}{\partial\tilde{\theta}}\right)+\left(\frac{D}{L}\right)^2\frac{\partial}{\partial\bar{z}}\left(3h_0^2\cos\tilde{\theta}\frac{\partial\bar{p}_0}{\partial\bar{z}}\right)= \\ &=12\pi\frac{\partial h_0}{\partial\tilde{\theta}}\left(\frac{3\cos\tilde{\theta}}{h_0}\right)+3h_0^3\frac{\partial\bar{p}_0}{\partial\tilde{\theta}}\frac{\partial}{\partial\tilde{\theta}}\left(\frac{\cos\tilde{\theta}}{h_0}\right) \end{aligned}$$

Thus, the following set of equations is obtained for the pressure field and the steady state pressure field gradients.

$$\frac{\partial}{\partial\tilde{\theta}}\left(h_0^3\frac{\partial\bar{p}_0}{\partial\tilde{\theta}}\right)+\left(\frac{D}{L}\right)^2\frac{\partial}{\partial\bar{z}}\left(h_0^3\frac{\partial\bar{p}_0}{\partial\bar{z}}\right)=12\pi\frac{\partial h_0}{\partial\tilde{\theta}}$$

ISSN-On line: 2410-4191

$$\frac{\partial}{\partial\tilde{\theta}}\left(h_0^3\frac{\partial\bar{p}_X}{\partial\tilde{\theta}}\right)+\left(\frac{D}{L}\right)^2\frac{\partial}{\partial z}\left(h_0^3\frac{\partial\bar{p}_X}{\partial z}\right)=$$
$$=12\pi\left(\cos\tilde{\theta}-\frac{3\sin\tilde{\theta}}{h_0}\frac{\partial h_0}{\partial\tilde{\theta}}\right)-3h_0^3\frac{\partial\bar{p}_0}{\partial\tilde{\theta}}\frac{\partial}{\partial\tilde{\theta}}\left(\frac{\sin\tilde{\theta}}{h_0}\right)$$
$$\frac{\partial}{\partial\tilde{\theta}}\left(h_0^3\frac{\partial\bar{p}_Y}{\partial\tilde{\theta}}\right)+\left(\frac{D}{L}\right)^2\frac{\partial}{\partial z}\left(h_0^3\frac{\partial\bar{p}_Y}{\partial z}\right)=$$
$$=-12\pi\left(\sin\tilde{\theta}+\frac{3\cos\tilde{\theta}}{h_0}\frac{\partial h_0}{\partial\tilde{\theta}}\right)-3h_0^3\frac{\partial\bar{p}_0}{\partial\tilde{\theta}}\frac{\partial}{\partial\tilde{\theta}}\left(\frac{\cos\tilde{\theta}}{h_0}\right)$$
$$\frac{\partial}{\partial\tilde{\theta}}\left(h_0^3\frac{\partial\bar{p}_{X'}}{\partial\tilde{\theta}}\right)+\left(\frac{D}{L}\right)^2\frac{\partial}{\partial\bar{z}}\left(h_0^3\frac{\partial\bar{p}_{X'}}{\partial\bar{z}}\right)=24\pi\sin\tilde{\theta}$$
$$\frac{\partial}{\partial\tilde{\theta}}\left(h_0^3\frac{\partial\bar{p}_{Y'}}{\partial\tilde{\theta}}\right)+\left(\frac{D}{L}\right)^2\frac{\partial}{\partial\bar{z}}\left(h_0^3\frac{\partial\bar{p}_{Y'}}{\partial\bar{z}}\right)=24\pi\cos\tilde{\theta} \qquad (24)$$

The boundary conditions associated with the system of equations given by (24) will be:

$p_l=0$ in $z=\pm L/2$; where $l=0,x,y,\dot{x},\dot{y}$

$\frac{\partial p_l}{\partial z}=0$ in $z=0$; where $l=0,x,y,\dot{x},\dot{y}$

Importantly for the aerodynamic coefficients through gradients $p_x$, $p_y$, $p_{\dot{x}}$ and $p_{\dot{y}}$, you need to calculate the first steady-state pressure $p_0$. The accuracy when calculating $p_0$ lead to the accuracy of the values of the dynamic coefficients.

## Short Chumacera Case Analysis

To verify that the pressure field disturbances lead to correct numeric results dynamic coefficients for the case of infinitely short bearings are calculated.

Consider the two assumptions for short bearings made by Dubios and Ocvirk [5]. First, the pressure gradients in the x or $\theta$ are negligible when compared to the pressure gradients in the direction *z* (axial direction). Second, only the pressure in the convergent region clear ($0 < \theta < \pi$) It is considered for evaluating forces lubricant film.

Therefore, in the case of short bearings, equations (24) reduce to the following expressions. $\left(\frac{D}{L}\right)^2\frac{\partial}{\partial\bar{z}}\left(h_0^3\frac{\partial\bar{p}_0}{\partial\bar{z}}\right)=12\pi\frac{\partial h_0}{\partial\tilde{\theta}}$

$$\left(\frac{D}{L}\right)^2\frac{\partial}{\partial\bar{z}}\left(h_0^3\frac{\partial\bar{p}_X}{\partial\bar{z}}\right)=12\pi\left(\cos\tilde{\theta}-\frac{3\sin\tilde{\theta}}{h_0}\frac{\partial h_0}{\partial\tilde{\theta}}\right)$$
$$\left(\frac{D}{L}\right)^2\frac{\partial}{\partial\bar{z}}\left(h_0^3\frac{\partial\bar{p}_Y}{\partial\bar{z}}\right)=-12\pi\left(\sin\tilde{\theta}+\frac{3\cos\tilde{\theta}}{h_0}\frac{\partial h_0}{\partial\tilde{\theta}}\right)$$
$$\left(\frac{D}{L}\right)^2\frac{\partial}{\partial\bar{z}}\left(h_0^3\frac{\partial\bar{p}_{X'}}{\partial\bar{z}}\right)=24\pi\sin\tilde{\theta}$$
$$\left(\frac{D}{L}\right)^2\frac{\partial}{\partial\bar{z}}\left(h_0^3\frac{\partial\bar{p}_{Y'}}{\partial\bar{z}}\right)=24\pi\cos\tilde{\theta} \qquad (25)$$

Note that the right side of the above equations is independent of the steady-state pressure $p_0$, as if it was in the system (24) for general bearings.

Integrating twice each of these equations and boundary conditions using established:

$$\bar{p}_0=\frac{(\bar{z}^2-1)}{2h_0^3}\left(\frac{L}{D}\right)^2\left[12\pi\frac{\partial h_0}{\partial\tilde{\theta}}\right]$$
$$\bar{p}_X=\frac{(\bar{z}^2-1)}{2h_0^3}\left(\frac{L}{D}\right)^2\left[12\pi\left(\cos\tilde{\theta}-\frac{3\sin\tilde{\theta}}{h_0}\frac{\partial h_0}{\partial\tilde{\theta}}\right)\right]$$
$$\bar{p}_Y=\frac{(\bar{z}^2-1)}{2h_0^3}\left(\frac{L}{D}\right)^2\left[-12\pi\left(\sin\tilde{\theta}+\frac{3\cos\tilde{\theta}}{h_0}\frac{\partial h_0}{\partial\tilde{\theta}}\right)\right]$$
$$\bar{p}_{X'}=\frac{(\bar{z}^2-1)}{2h_0^3}\left(\frac{L}{D}\right)^2\left[24\pi\sin\tilde{\theta}\right]$$
$$\bar{p}_{Y'}=\frac{(\bar{z}^2-1)}{2h_0^3}\left(\frac{L}{D}\right)^2\left[24\pi\cos\tilde{\theta}\right] \qquad (26)$$

Known $p_0$ and pressure gradients, the reaction forces and dynamic coefficients are calculated. In dimensionless form can be written:

$$\bar{F}_x=\frac{1}{4}\int_{-1}^{1}\int_{\phi}^{\phi+\pi}\bar{p}_0\sin\tilde{\theta}\,d\theta d\bar{z} \qquad \bar{F}_y=\frac{1}{4}\int_{-1}^{1}\int_{\phi}^{\phi+\pi}\bar{p}_0\cos\tilde{\theta}\,d\theta d\bar{z}$$
$$\bar{k}_{xx}=\frac{1}{4}\int_{-1}^{1}\int_{\phi}^{\phi+\pi}\bar{p}_X\sin\tilde{\theta}\,d\theta d\bar{z} \qquad \bar{k}_{xy}=\frac{1}{4}\int_{-1}^{1}\int_{\phi}^{\phi+\pi}\bar{p}_Y\sin\tilde{\theta}\,d\theta d\bar{z}$$
$$\bar{k}_{yx}=\frac{1}{4}\int_{-1}^{1}\int_{\phi}^{\phi+\pi}\bar{p}_X\cos\tilde{\theta}\,d\theta d\bar{z} \qquad \bar{k}_{yy}=\frac{1}{4}\int_{-1}^{1}\int_{\phi}^{\phi+\pi}\bar{p}_Y\cos\tilde{\theta}\,d\theta d\bar{z}$$

ISSN-On line: 2410-4191

$$\bar{c}_{xx}=\frac{\omega}{4}\int_{-1}^{1}\int_{\phi}^{\phi+\pi}\bar{p}_{X'}\sin\tilde{\theta}\,d\theta d\bar{z}\quad \bar{c}_{xy}=\frac{1}{4}\int_{-1}^{1}\int_{\phi}^{\phi+\pi}\bar{p}_{Y'}\sin\tilde{\theta}\,d\theta d\bar{z}$$

$$\bar{c}_{yx}=\frac{1}{4}\int_{-1}^{1}\int_{\phi}^{\phi+\pi}\bar{p}_{X'}\cos\tilde{\theta}\,d\theta d\bar{z}\quad \bar{c}_{yy}=\frac{1}{4}\int_{-1}^{1}\int_{\phi}^{\phi+\pi}\bar{p}_{Y'}\cos\tilde{\theta}\,d\theta d\bar{z}$$

## Results

Evaluating each of these integrals it is obtained for the forces in the lubricant:

$$\begin{aligned}\bar{F}_X&=\frac{1}{4}\int_{-1}^{1}\int_{\phi}^{\phi+\pi}\frac{(\bar{z}^2-1)}{2h_0^3}\left(\frac{L}{D}\right)^2 12\pi\frac{\partial h_0}{\partial\tilde{\theta}}\sin\tilde{\theta}\,d\tilde{\theta}\,d\bar{z}\\&=-2\pi\left(\frac{L}{D}\right)^2\int_{\phi}^{\phi+\pi}\frac{\partial h_0}{\partial\tilde{\theta}}\frac{\sin\tilde{\theta}}{h_0^3}d\tilde{\theta}\\&=2\pi\left(\frac{L}{D}\right)^2\int_0^{\pi}\frac{\varepsilon\sin\theta}{(1+\varepsilon\cos\theta)^3}\sin(\theta+\phi)d\theta\\&=2\pi\left(\frac{L}{D}\right)^2\left[\frac{\pi\varepsilon}{2(1-\varepsilon^2)^{3/2}}\cos\phi-\frac{2\varepsilon^2}{(1-\varepsilon^2)^2}\sin\phi\right]=0\end{aligned}\tag{27}$$

$$\begin{aligned}\bar{F}_Y&=\frac{1}{4}\int_{-1}^{1}\int_{\phi}^{\phi+\pi}\frac{(\bar{z}^2-1)}{2h_0^3}\left(\frac{L}{D}\right)^2 12\pi\frac{\partial h_0}{\partial\tilde{\theta}}\cos\tilde{\theta}\,d\tilde{\theta}\,d\bar{z}\\&=2\pi\left(\frac{L}{D}\right)^2\left[\frac{-2\varepsilon^2}{(1-\varepsilon^2)^2}\cos\phi-\frac{\pi\varepsilon}{2(1-\varepsilon^2)^{3/2}}\sin\phi\right]\\&=\frac{-\varepsilon\pi}{(1-\varepsilon^2)^2}\left(\frac{L}{D}\right)^2\sqrt{16\varepsilon^2+\pi^2(1-\varepsilon^2)}\end{aligned}\tag{28}$$

Dynamic stiffness coefficients are obtained as follows:

$$\begin{aligned}\bar{k}_{xx}&=\frac{1}{4}\int_{-1}^{1}\int_{\phi}^{\phi+\pi}\frac{(\bar{z}^2-1)}{2h_0^3}\left(\frac{L}{D}\right)^2\left[12\pi\left(\cos\tilde{\theta}-\frac{3\sin\tilde{\theta}}{h_0}\frac{\partial h_0}{\partial\tilde{\theta}}\right)\right]\sin\tilde{\theta}\,d\tilde{\theta}\,d\bar{z}\\&=2\pi\left(\frac{L}{D}\right)^2\left[\frac{2\varepsilon}{(1-\varepsilon^2)^2}\cos^2\phi-\frac{3\pi\varepsilon^2}{2(1-\varepsilon^2)^{5/2}}\sin\phi\cos\phi+\frac{4\varepsilon(1+\varepsilon^2)}{(1-\varepsilon^2)^3}\sin^2\phi\right]\\&=\pi\left(\frac{L}{D}\right)^2\frac{4\varepsilon}{(1-\varepsilon^2)^2}\frac{2\pi^2+(16-\pi^2)\varepsilon^2}{16\varepsilon^2+\pi^2(1-\varepsilon^2)}\end{aligned}\tag{29}$$

$$\begin{aligned}\bar{k}_{xy}&=\frac{1}{4}\int_{-1}^{1}\int_{\phi}^{\phi+\pi}\frac{(\bar{z}^2-1)}{2h_0^3}\left(\frac{L}{D}\right)^2\left[-12\pi\left(\sin\tilde{\theta}+\frac{3\cos\tilde{\theta}}{h_0}\frac{\partial h_0}{\partial\tilde{\theta}}\right)\right]\sin\tilde{\theta}\,d\tilde{\theta}\,d\bar{z}\\&=2\pi\left(\frac{L}{D}\right)^2\left[\frac{-\pi(1+2\varepsilon^2)}{2(1-\varepsilon^2)^{5/2}}\cos^2\phi+\frac{2\varepsilon(1+3\varepsilon^2)}{(1-\varepsilon^2)^3}\sin\phi\cos\phi-\frac{\pi}{2(1-\varepsilon^2)^{3/2}}\sin^2\phi\right]\\&=\pi\left(\frac{L}{D}\right)^2\frac{1}{(1-\varepsilon^2)^{5/2}}\frac{\pi[-\pi^2+2\pi^2\varepsilon^2+(16-\pi^2)\varepsilon^4]}{16\varepsilon^2+\pi^2(1-\varepsilon^2)}\end{aligned}\tag{30}$$

$$\begin{aligned}\bar{k}_{yx}&=\frac{1}{4}\int_{-1}^{1}\int_{\phi}^{\phi+\pi}\frac{(\bar{z}^2-1)}{2h_0^3}\left(\frac{L}{D}\right)^2\left[12\pi\left(\cos\tilde{\theta}-\frac{3\sin\tilde{\theta}}{h_0}\frac{\partial h_0}{\partial\tilde{\theta}}\right)\right]\cos\tilde{\theta}\,d\tilde{\theta}\,d\bar{z}\\&=2\pi\left(\frac{L}{D}\right)^2\left[\frac{\pi}{2(1-\varepsilon^2)^{3/2}}\cos^2\phi+\frac{2\varepsilon(1+3\varepsilon^2)}{(1-\varepsilon^2)^3}\sin\phi\cos\phi+\frac{\pi(1+2\varepsilon^2)}{2(1-\varepsilon^2)^{5/2}}\sin^2\phi\right]\\&=2\pi\left(\frac{L}{D}\right)^2\frac{\pi[\pi^2+(32+\pi^2)\varepsilon^2+2(16-\pi^2)\varepsilon^4]}{2(1-\varepsilon^2)^{5/2}[16\varepsilon^2+\pi^2(1-\varepsilon^2)]}\end{aligned}\tag{31}$$

$$\begin{aligned}\bar{k}_{yy}&=\frac{1}{4}\int_{-1}^{1}\int_{\phi}^{\phi+\pi}\frac{(\bar{z}^2-1)}{2h_0^3}\left(\frac{L}{D}\right)^2\left[-12\pi\left(\sin\tilde{\theta}+\frac{3\cos\tilde{\theta}}{h_0}\frac{\partial h_0}{\partial\tilde{\theta}}\right)\right]\cos\tilde{\theta}\,d\tilde{\theta}\,d\bar{z}\\&=2\pi\left(\frac{L}{D}\right)^2\left[\frac{4\varepsilon(1+\varepsilon^2)}{(1-\varepsilon^2)^3}\cos^2\phi+\frac{3\pi\varepsilon^2}{2(1-\varepsilon^2)^{5/2}}\sin\phi\cos\phi+\frac{2\varepsilon}{(1-\varepsilon^2)^2}\sin^2\phi\right]\\&=\pi\left(\frac{L}{D}\right)^2\frac{4\varepsilon[\pi^2+(32+\pi^2)\varepsilon^2+2(16-\pi^2)\varepsilon^4]}{(1-\varepsilon^2)^3[16\varepsilon^2+\pi^2(1-\varepsilon^2)]}\end{aligned}\tag{32}$$

Damping coefficients are:

$$\begin{aligned}\bar{c}_{xx}&=\frac{1}{4}\int_{-1}^{1}\int_{\phi}^{\phi+\pi}\frac{(\bar{z}^2-1)}{2h_0^3}\left(\frac{L}{D}\right)^2\left[24\pi\sin\tilde{\theta}\right]\sin\tilde{\theta}\,d\tilde{\theta}\,d\bar{z}\\&=4\pi\left(\frac{L}{D}\right)^2\left[\frac{\pi}{2(1-\varepsilon^2)^{3/2}}\cos^2\phi-\frac{4\varepsilon}{(1-\varepsilon^2)^2}\sin\phi\cos\phi+\frac{\pi(1+2\varepsilon^2)}{2(1-\varepsilon^2)^{5/2}}\sin^2\phi\right]\\&=2\pi\left(\frac{L}{D}\right)^2\left[\frac{\pi[\pi^2+2(\pi^2-8)\varepsilon^2]}{(1-\varepsilon^2)^{3/2}[16\varepsilon^2+\pi^2(1-\varepsilon^2)]}\right]\end{aligned}\tag{33}$$

$$\begin{aligned}\bar{c}_{xy}=\bar{c}_{yx}&=\frac{1}{4}\int_{-1}^{1}\int_{\phi}^{\phi+\pi}\frac{(\bar{z}^2-1)}{2h_0^3}\left(\frac{L}{D}\right)^2\left[24\pi\cos\tilde{\theta}\right]\sin\tilde{\theta}\,d\tilde{\theta}\,d\bar{z}\\&=4\pi\left(\frac{L}{D}\right)^2\left[\frac{-2\varepsilon}{(1-\varepsilon^2)^2}\cos^2\phi+\frac{3\pi\varepsilon^2}{2(1-\varepsilon^2)^{5/2}}\sin\phi\cos\phi+\frac{2\varepsilon}{(1-\varepsilon^2)^2}\sin^2\phi\right]\\&=\pi\left(\frac{L}{D}\right)^2\left[\frac{8\varepsilon[\pi^2+2(\pi^2-8)\varepsilon^2]}{(1-\varepsilon^2)^2[16\varepsilon^2+\pi^2(1-\varepsilon^2)]}\right]\end{aligned}\tag{34}$$

$$\begin{aligned}\bar{c}_{yy}&=\frac{1}{4}\int_{-1}^{1}\int_{\phi}^{\phi+\pi}\frac{(\bar{z}^2-1)}{2h_0^3}\left(\frac{L}{D}\right)^2\left[24\pi\cos\tilde{\theta}\right]\cos\tilde{\theta}\,d\tilde{\theta}\,d\bar{z}\\&=4\pi\left(\frac{L}{D}\right)^2\left[\frac{\pi(1+2\varepsilon^2)}{2(1-\varepsilon^2)^{5/2}}\cos^2\phi+\frac{4\varepsilon}{(1-\varepsilon^2)^2}\sin\phi\cos\phi+\frac{\pi}{2(1-\varepsilon^2)^{3/2}}\sin^2\phi\right]\\&=2\pi\left(\frac{L}{D}\right)^2\left[\frac{\pi[\pi^2+2(24-\pi^2)\varepsilon^2+\pi^2\varepsilon^4]}{(1-\varepsilon^2)^{5/2}[16\varepsilon^2+\pi^2(1-\varepsilon^2)]}\right]\end{aligned}\tag{35}$$

Tables 1 and 2 show these coefficients in the form $\tilde{k}_{ij}=(C/W)k_{ij}$ y $\tilde{c}_{ij}=(\omega C/W)c_{ij}$.

ISSN-On line: 2410-4191


RAMIREZ, Ignacio, CANO, Alexis and ANTONIO, Alberto. The method of small perturbations to Calculate Stiffness and damping in a Short Chumacera. ECORFAN Journal-Bolivia 2015.

| |
|---|
| $\tilde{k}_{xx} = \frac{4[2\pi^2 + (16-\pi^2)\varepsilon^2]}{[\pi^2 + (16-\pi^2)\varepsilon^2]^{3/2}}$ |
| $\tilde{k}_{xy} = \frac{\pi[-\pi^2 + 2\pi^2\varepsilon^2 + (16-\pi^2)\varepsilon^4]}{\varepsilon\sqrt{1-\varepsilon^2}[\pi^2 + (16-\pi^2)\varepsilon^2]^{3/2}}$ |
| $\tilde{k}_{yx} = \frac{\pi[\pi^2 + (32+\pi^2)\varepsilon^2 + 2(16-\pi^2)\varepsilon^4]}{\varepsilon\sqrt{1-\varepsilon^2}[\pi^2 + (16-\pi^2)\varepsilon^2]^{3/2}}$ |
| $\tilde{k}_{yy} = \frac{4[\pi^2 + (32+\pi^2)\varepsilon^2 + 2(16-\pi^2)\varepsilon^4]}{(1-\varepsilon^2)[\pi^2 + (16-\pi^2)\varepsilon^2]^{3/2}}$ |

**Table 1** Dynamic stiffness coefficients for a short bearing.

| |
|---|
| $\tilde{c}_{xx} = \frac{2\pi(1-\varepsilon^2)^{1/2}[\pi^2 + 2(\pi^2-8)\varepsilon^2]}{\varepsilon[\pi^2 + (16-\pi^2)\varepsilon^2]^{3/2}}$ |
| $\tilde{c}_{xy} = \frac{8[\pi^2 + 2(\pi^2-8)\varepsilon^2]}{[\pi^2 + (16-\pi^2)\varepsilon^2]^{3/2}}$ |
| $\tilde{c}_{yx} = \frac{8[\pi^2 + 2(\pi^2-8)\varepsilon^2]}{[\pi^2 + (16-\pi^2)\varepsilon^2]^{3/2}}$ |
| $\tilde{c}_{yy} = \frac{2\pi[\pi^2 + 2(24-\pi^2)\varepsilon^2 + \pi^2\varepsilon^4]}{\varepsilon\sqrt{1-\varepsilon^2}[\pi^2 + (16-\pi^2)\varepsilon^2]^{3/2}}$ |

**Table 2** Dynamic damping coefficients for a short bearing.

You can view the behavior of these coefficients as a function of the eccentricity of balance. In Figures 3 and 4 the damping and stiffness variations appear; the dashed curves correspond to negative values of the coefficient.

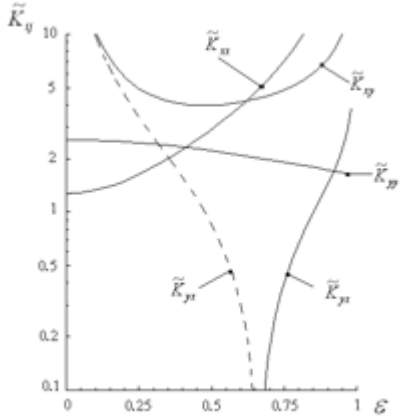


**Figure 3** aerodynamic coefficients for a short Chumacera stiffness.

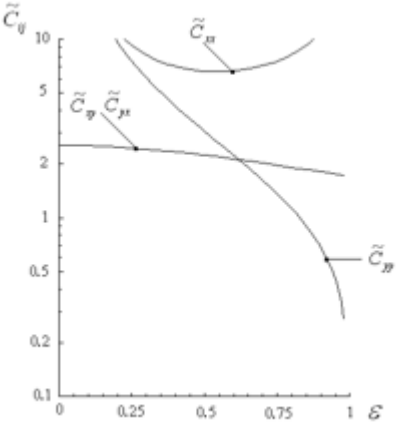


**Figure 4** aerodynamic damping coefficients for a short Chumacera.

As noted, the coefficients obtained for the classical case are the same as they find alternatives [3] methodologies [4], [10]; meaning that the alternate method produces consistent results.

## Conclusions

After showing the validity of this alternative solution, you might expect the perturbation technique can be used in more complex analysis that may involve external excitations in the bearings, the eternal problem of misalignment in the stands, and an option to open external pressurization ports lubricant.

ISSN-On line: 2410-4191


RAMIREZ, Ignacio, CANO, Alexis and ANTONIO, Alberto. The method of small perturbations to Calculate Stiffness and damping in a Short Chumacera. ECORFAN Journal-Bolivia 2015.

Currently there are rough on some of these issues results but the perturbation technique can be adapted to become a numerical-analytical methodology to find rotordynamic coefficients as a function of misalignment and external pressurization bearings of any length.

**References**

Childs, D. (1993), "Turbomachinery Rotordynamics Phenomena, Modeling, and Analysis," A Wiley-Interescience Publication, John Wiley and Sons, Inc.

Hamrock B. Fundamentals of Fluid Film Lubrication, Mc Graw Hill. 1994

Antonio-García, Valery R. Nossov, Gómez-Mancilla J.C.,(2001), "Comparación de Coeficientes Rotodinámicos de Chumaceras Hidrodinámicas Usando la Teoría de Chumaceras Largas, Cortas y Warner," 3er Congreso Internacional de Ingeniería Electromecánica y Sistemas, IM-D-21 pag. 106-111, Noviembre 2002, México, D.F.

Szeri, A. Z., (1998) "Fluid Film Lubrication," Cambridge University Press.

Dubois, G. B. and Ocvirk, E. W. (1953), "Analytical Derivation and Experimental Evaluation of Short Bearing Approximation for Full Journal Bearings," NACA Report 1157

Tower, B. (1883), "Second Report on Friction Experiments," Proc. Inst. Mech. Engrs., Vol 36, pp. 58-70

Reynolds, O. (1886), "On the Theory of Lubrication and its Application to Mr. Beauchamp Tower's Experiments, Including an Experimental Determination of the Viscosity of Olive Oil," Phil. Trans. Roy. Soc., London, Vol. 177, Part I, pp. 157-234.

Harnoy, A. (2003), "Bearing Design in Machinery, Engineering Tribology and Lubrication," Marcel Dekker, Inc.

Lund, J., and Sternlicht, B. (1962), "Rotor-Bearing Dynamics with Emphasis on Attenuation," ASME Trans. Journal of Basic Engineering, Ser. D, 84, 491-502.

Ramírez Vargas, I. Teoría de chumaceras presurizadas con puertos puntuales. Caso de la chumacera corta. Instituto Politécnico Nacional, México D.F. 2007

ISSN-On line: 2410-4191

Article ECORFAN Journal
FOOD TECHNOLOGY June 2015 Vol.2 No.2 118-125

# Evaluation of antibacterial activity of essential oil Origanum vulgare (oregano)

SANDOVAL, Francisca*†, DOMINGUEZ, Maricela, CONTRERAS, Raúl and REYES, Coral

Received January 8, 2014; Accepted June 12, 2015

## Abstract

The aim of the research is to evaluate the antibacterial activity of the essential oil of Origanum vulgare (oregano) against pathogenic bacteria to man. Methodology: The essential oil is obtained by maceration of leaves and stems, then purified by filtration assisted distillation separated by rotavapor, the chemical characterization was determined by HPLC and FTIR spectroscopy. The antibacterial evaluation was made by the diffusion method on agar plates against Gram positive (Staphylococcus aureus) and Gram negative bacteria (Escherichia coli, Proteus mirabilis and Klepsiella pneumoniae) using dilutions of 1:10, 1: 100 and 100% of essential oil of oregano. Results: The chromatogram confirming the presence of thymol, carvacrol, ferulic acid and caffeic acid latter two greater intensity responsible for the antibacterial and antioxidant activities. FTIR spectroscopy study by the presence of group's functions as phenols, alcohols and carboxylic acids were identified. The bacteria tested showed sensitivity in dilutions of 1:10, in determining the minimum bactericidal concentration (MBC) showed greater inhibition in microdilutions 1: 100 Essential oil to positive gram-negative bacteria. Conclusion: The essential oil has bacteriostatic and bactericidal activity against bacteria tested showing different degrees of sensitivity.

**Antimicrobial, Evaluation, metabolite.**

**Citation:** SANDOVAL, Francisca, DOMINGUEZ, Maricela, CONTRERAS, Raúl and REYES, Coral. Evaluation of antibacterial activity of essential oil Origanum vulgare (oregano). ECORFAN Journal-Bolivia 2015, 2-2: 118-125

* Correspondence to Author (email: sanrey_10@hotmail.com)
† Researcher contributing first author.

 

## Introduction

Today has increased the search for natural ingredients to replace synthetic substances which mostly can be harmful to health. Essential oils of plants are mixtures of several chemicals that can be used in industries perfumes, soaps, disinfectants and similar products.

Oregano is a wild aromatic plant since ancient times is used as a seasoning in various dishes; Arcila Garcia as 2003 and 2013 have shown that according to their chemical composition can be used in the pharmaceutical industry, in Mexico more than 40 species of oregano are known, however it is grown mostly for export purposes.

The essential oil of Origanum vulgare (oregano) on its chemical composition has thymol and carvacrol (Garcia 2013), which according to studies are responsible for antibacterial activity. (Davidson and Naidu 2000).

## General oregano

Origanum vulgare its botanical name, which derives from Greek, "splendor of the mountain." It is a native plant to Central Europe, South and Central Asia. The Spanish introduced the country oregano around 1970 in the central area, where later was grown extensively (Ávila-Sosa
2008).

In the international market Turkey, Greece and Mexico are the main suppliers of dried oregano manufactured and not manufactured in the world, however, Turkey and Mexico provide 65 to 31% of production respectively the rest of the production bring other countries Mediterranean.

## Essential oil

Essential oils are used as therapeutic agents, because of its smell and flavor, many others were used as key ingredients in the industries of perfumes, soaps, disinfectants and similar products. In the food industry they are extensively used as flavoring in a wide variety of food and drink (Holley and Patel, 2005).

They have shown that the essential oil of Origanum vulgare (oregano) has activity against the gam-negative bacteria: Escherichia coli, Salmonella typhimurium, Vibrio cholerae, Klebsiella pneumoniae, Proteus mirabilis and gram-positive bacteria: Staphylococcus with different degrees of sensitivity (Albado, 2001).

## Chemical composition

There are several studies on the chemistry of oregano, using aqueous extracts and oils essential. Flavonoids have been identified as apigenin and luteolin, aliphatic alcohols, terpenes and compounds derived phenylpropane (Dardioi, 1997).

In Origanum vulgare they found coumerico acid, ferulic, caffeic, r -hydroxybenzoic and vanillin. The essential oils of Lippia species containing limonene, -cariofilene b, r -cymene, camphor, linalool, a-pinene and thymol, which can vary according to chemotype.

Thymol and carvacrol are natural phenolic compounds considered as potential antioxidants, antifungal and antibacterial agents, present in significant amounts in essential oils and Lippia Origanum genus, species widely used as spices and herbal teas (Burdock, 2005).

ISSN-On line: 2410-4191

### Uses and properties

One of the most common uses for oregano is as relish typical dishes of each country (Aranda Ruiz et al., 2009). In Mexico, it is used as a spice for flavoring and as a preservative in various fresh and processed foods of national and international dishes numbers (Huerta, 1997).

In traditional medicine, the infusion of the leaves is used for the treatment of skin infections, anti-fungal, respiratory diseases, cough, bronchitis, fever and amenorrhea problems to regulate menstruation and hepatic disorders such as diuretic, antihypertensive and antimicrobial, as repellent, abortion, and local anesthetic perspiratory (Arcila Lozano et al., 2007).

The essential oil extracted from oregano leaf is used in the soft drink industry, liquor, pharmaceutical and cosmetology (FAO 2000), as well as in the preparation of soaps and aromatherapy products (Sanchez et al., 2007) and for the production of oil for aeronautics and automotive parts cleaning, and making candles (SEMARNAT, 2007).

### Methodology

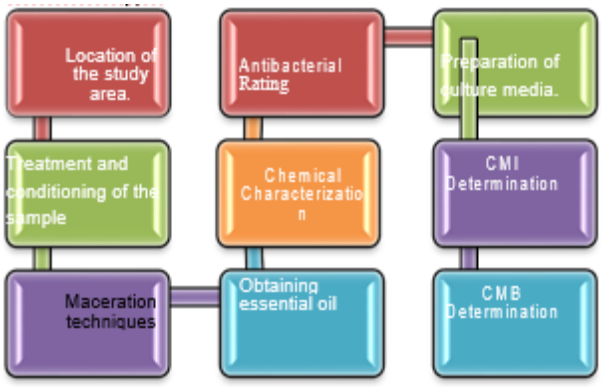


### Location of the study area

The Origanum vulgare serves as an object of study is collected in the community of Karistay Papantla municipality located in the north-central state of Veracruz part.

### Treatment and conditioning of the sample

The collected Origanum vulgare plants are washed with water to remove dirt that may contain, after the washing process a selection of leaves and stems that are in good condition subsequently smaller parts is reduced by a grinding process is performed mechanic.

### Maceration

The sample C is placed to sun exposure for drying the same for a period of about two weeks at a temperature of 35 °. After drying the sample, placed in a container with cane alcohol 25 ° marinate for three weeks to extract the secondary metabolites.

Oil extraction assisted by distillation method (Broken steam). 400 mL of the mash at 80 rpm solution are placed 55C, obtaining 5% of essential oil of oregano, with a time of two hours.

Once the essential oil is obtained is necessary to filter to purify it, then deposit it in a glass bottle amber and place it in a cool environment to avoid degradation by the effects of light, moisture absorption, evaporation of volatile constituents, oxidation by air and changes due to the action of microorganisms.

### HPLC chromatography

A sample of 5 mL of Origanum vulgare essential oil is taken and brought to the facilities of Nanoscience and Nanotechnology Micro and IPN for analysis by HPLC. procedure:

ISSN-On line: 2410-4191

1. They should be substances with a HPLC purity.

2. They should be filtered with filters of pore diameters about 20 .mu.m and 45μm.

3. You have to wash the tubes that contain the sample with HPLC grade deionized water.

4. Purge to homogenize the column and no a mobile phase residues from an above experiment to ensure that the separated compounds are solely those we add to the machine.

**Transform infrared spectrophotometry**

**FTIR Fourier**

A sample of 5 mL of essential oil of oregano is taken and brought to the facilities of Nanoscience and Nanotechnology Micro and IPN for analysis by infrared spectrometry with Fourier Transform (FTIR). Procedure:

1. Preparation, offline sample in aqueous medium.

2. Introduction of the sample system.

3. Removing -in line- of Origanum vulgare essential oil to the organic phase and separating the organic and aqueous phases.

4. Acquisition FTIR spectrum.

5. Analysis of the spectra.

**Antibacterial Evaluation**

**Sterilization of laboratory equipment used.**

The pressure steam sterilization is performed in a autoclave.

This device uses saturated steam at 15 pounds pressure allowing the chamber reaches 121 ° C. The sterilization time is usually 15 minutes.

**Preparation of culture media.**

Petri dishes of 9 cm in diameter are used for 1 cm, which is added 20 mL of nutrient agar solid basis. 5 species of bacteria obtained from the microbiology laboratory of the IMSS regional hospital in Poza Rica de Hidalgo, View assessed. Which are Staphylococcus aureus, Escherichia coli, Klebsiella pneumoniae and Proteus mirabilis.

**Planting strain**

With the previously sterile loop, taking a hoe a sample and plot grooves closest to each other inside the box with the culture medium used subsequently incubated in bacteriological stove, in a period of 24 to 48 hours at a constant temperature of 36 ° C.

**Preparation of oil dilution.**

Dilutions of essential oil and ethyl alcohol according to the following concentrations 1:10, 1 are used: 100 and 100% for each evaluated using sensidiscs bacteria cellulose, leaving to incubate for 48 hours at a temperature of 37 ° C, analyzing results every 24 hours.

**Bacteriostatic and bactericidal evaluation.**

Once the seed and placed in the sensidiscs bacteria incubated and take two readings of the know (24 and 48 hours) to determine the presence of inhibition zones (lysis) and thus show the antimicrobial activity of oil as shown in the Table 1.

ISSN-On line: 2410-4191

**Determination of minimum inhibitory concentration (CMI)**

This technique incorporates the essential oil of Origanum vulgare (antimicrobial) to sensidiscs filter paper. Introduction allows determination of the inhibition of the bacterial strains.

Investigating the pathogenic bacterium it is inoculated into one or more agar plates and on the surface thereof impregnated sensidiscs of different dilutions made above are introduced.

The plates were incubated for 24 and 48 hours and growth is analyzed therein. The diameter of the inhibition zone formed around each disc is evaluated.

In this way you know if the pathogenic bacteria is sensitive, intermediate or resistant to each of the solutions, for this study the symbols shown in the table was used.

| Sensitive | Intermediate | Resistant |
|---|---|---|
| + | ++ | - |

**Table 1** Bacterial inhibition

**Determination of minimum bactericidal concentration (MBC)**

Its objective is to determine the lowest concentration of an antimicrobial that is able to kill a bacterial strain, in order to compare it with that reached in a given location.

**Procedure**:

1. Perform microdilutions 1:10 and 1: 100 for essential oil of Origanum vulgare, alcohol as solvent.

2. Enter within the sensidiscs microdilutions filter paper.

3. Perform planting by massive groove of each bacteria in Mueller-Hinton agar and place 4 sensidiscs according to the clock hands.

4. Incubate in bacteriological stove for 24 hours at 36 ° C

5. Interpretation of results.

Determine if the microorganism is sensitive (+), Intermediate (++) or resistant (-) to each solution used during the study.

**Results**

**Location of the study area**

The raw material (Origanum vulgare) was collected in the community of Karistay town of Papantla, ., With coordinates Latitude 20 ° 38'26.15 "N, longitude 97 ° 18'29.54 "W; - Tuxpan (Microbiology Lab) collected material to the facilities of the University of Veracruz Poza Rica was carried Campus.

**Obtaining essential oil**

Method was used for maceration for extraction of secondary metabolites and for separation of the essential oil assisted distillation (broken steam) was used, was obtained with 400 mL of the mash solution (leaves and stems of oregano) 20 mL oil oregano essential having a yield of 5%.

**Chemical characterization**

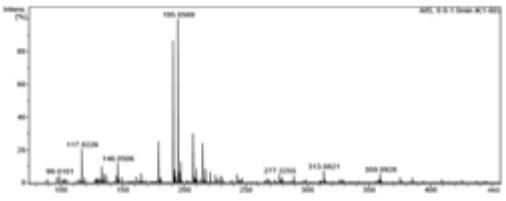

**Figure 1** Interpretation of HPLC Origanum vulgare essential oil.

ISSN-On line: 2410-4191

Figure 1 shows the components found in the essential oil of oregano molecular weights considering the presence of ferulic acid is inferred with an approximate molecular weight 05 to 195 gmol; Carvacrol and thymol with a molecular weight of 146.05 g / mol.

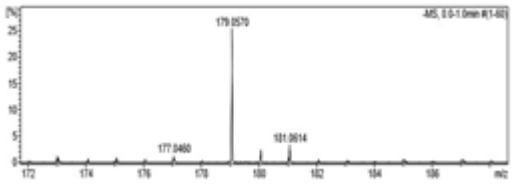

**Figure 2** Identification of caffeic acid.

Figure 2 highlights the presence of caffeic acid with a molecular weight of 179.05 and Dihidroactinidiolida with 181.06 g / mol, molecular weights approaching those found in the spectrum, so the presence of secondary metabolites oregano is confirmed.

## FTIR interpretation Origanum vulgare essential oil

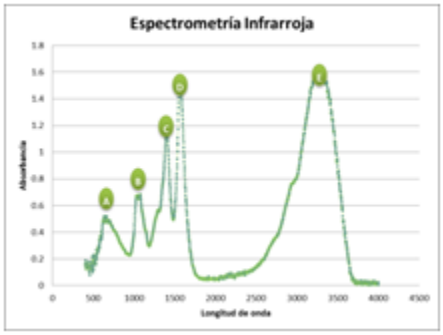


**Figure 3** Identification of secondary metabolites by ETIR

| absorbance | Functional group |
|---|---|
| A 624.89 $cm^{-1}$ | cycloalkanes |
| B 1024.76 $cm^{-1}$ | Fluoroalkanes / aliphatic amines |
| C 1393.00 $cm^{-1}$ | carboxylic acids |
| D 1560.38 $cm^{-1}$ | Carboxylic acids / Sales |
| E 323.06 $cm^{-1}$ | carboxylate / Amines |

**Table 2** Oregano functional groups by FTIR antibacterial evaluation

The bacteria were obtained through donation Clinical Laboratory Analysis Mexican Social Security Institute in the city of Poza Rica; which they were: Staphylococcus aureus, Proteus mirabilis, Escherichia coli, Klebsiella pneumoniae. Seeded each bacteria mentioned above in standard culture medium, subsequently reseeding was performed to purify.

## CMI determination of essential oil of oregano

| bacteria | inhibition<br>Sensible (+), Intermediate (++), Resistant (-) | | |
|---|---|---|---|
| Gram positive | 1:100 | 1:10 | 100% |
| Staphylococcus aureus | - | + | - |
| Gram negative | | | |
| Proteus mirabilis | + | + | + |
| Escherichia coli | - | + | ++ |
| Klebsiella pneumoniae | + | + | - |

**Table 3** Determination of oil CMI

ISSN-On line: 2410-4191

According to the assessment antibacterial essential oil of oregano has antibacterial activity to Staphylococcus aureus (gram positive) and Proteus mirabilis, Escherichia coli, Klebsilella pneumoniae (Gram negative) concentration 1:10. Table 4.

**CMB determination of essential oil of oregano**

| bacteria | microdilutions | |
|---|---|---|
| Gram positive | 1:100 | 1:10 |
| Staphylococcus aureus | ++ | + |
| Gram negative | | |
| Proteus mirabilis | ++ | + |
| Escherichia coli | + | - |
| Klebsiella pneumoniae | ++ | + |

**Table 4** Determination of OMB According to the evaluation of the minimum bactericidal concentration (MBC)

Table 4 is presented in Table oregano essential oil has antibacterial activity, using microdilutions to Staphylococcus aureus (gram positive) and Proteus mirabilis, Escherichia coli, Klebsiella pneumoniae negative). The concentration of 1: 100 exhibits greater inhibition against all strains tested.

## Conclusions

Based on the results obtained it is concluded that the method of extraction by maceration of the essential oil of oregano (Origanum vulgare) was ineffective showing a 5% yield.

The characterization study using HPLC and FTIR spectroscopy confirmed the presence of thymol and carvacrol, responsible for the antimicrobial properties of oregano.

Compared to the 2013 study by García components are found in greater intensity ferulic acid and caffeic acid.

**In the analysis of the Minimum Inhibitory**

**Concentration**

(CMI) has inhibitory results dilutions 1:10 Staphylococcus aureus and gram-negative bacteria Escherichia coli, Proteus mirabilis and Klepsiella pneumoniae.

In the analysis of the minimum bactericidal concentration (MBC) with the use of microdilutions 1: 100 Essential oil increased bacterial inhibition with gram positive bacteria Staphylococcus aureus and gram-negative bacteria Escherichia coli, Proteus mirabilis and Klepsiella pneumoniae was presented.
The essential oil of oregano finally concluded that the microbiological evaluation gives bacteriostatic and bactericidal activity with greater intensity as small dilutions shown inhibitory effects.

## Referencies

Albado E, Sáez G, Gabriel S. 2001. Composición química y actividad antibacteriana del aceite esencial del Origanum vulgare (orégano). Rev Med Hered 12 (1), 2001 (Rev Med Hered 2001; 12: 16-19).

Burt S. 2004. Essential oils: their antibacterial properties and potential applications in foods - a review. International Journal of Food Microbiology. 94. 223– 253.

Davidson PM, Naidu AS. 2000. Phyto-Phenols. In: Naidu, A.S. (Ed.), Natural Food Antimicrobial Systems. CRC Press, Boca Ratón, FL, pp. 265-294.

ISSN-On line: 2410-4191

Cela, R., R. A. Lorenzo, et al. (2002). Técnicas de separación en química analítica. Madrid, Editorial Síntesis.

Rzedowki, J. y G. Calderon. 2002. FAMILIA VERBENACEAE. Fascículo 100. Flora del bajío y de regiones adyacentes. Instituto de Ecología A.C. Centro Regional del Bajío. Conacyt y CONABIO, México.

Andrews MJ. Determination of Minimum Inhibitory Concentration. J Antimicrob Chemother 2001

Sanchez, O., Medellin, A. Aldama, B. Goettsch, J. Soberon 2007. Capítulo 8 "Evaluación del riesgo de extinción de Lippia graveolens de acuerdo al numeral 5.7 de la NOM-058-SEMARNAT-2001".

Flores, J. E., Percepción remota de contaminantes atmosféricos mediante dos métodos espectroscópicos en la zona centro de la Ciudad de México: FTIR y DOAS, tesis Maestría (Maestría en Ciencias de la Tierra)-UNAM, Centro de Ciencias de la Atmosfera, 2003.

Callejas T., Pablo A. Obtención de extractos de plantas en medios ácidos y/o alcohólicos para aplicaciones medicinales y alimenticias. Tesis. Universidad Nacional de Colombia. Manizales. 2002

González, V. Ángela A. Obtención de aceites esenciales y extractos etanólicos de plantas del Amazonas. Tesis. Universidad Nacional de Colombia. Manizales. 2004.

Madigan, M., Parker, J. 2002. Brock. Biología de los microorganismos. Décima Edición. Ed. Pearson.

Romero C, Raúl. Microbiología y parasitología humana: bases etiológicas de las enfermedades infecciosas y parasitarias. Tercera Edición. Editorial Médica Panamericana, 2007.

Villavicencio G., E., O. U. Martínez B. Y A. Cano P. 2005. OREGANO Recurso con alto potencial. Rev. Ciencia y Desarrollo.

ISSN-On line: 2410-4191

Article ECORFAN Journal
ANATOMY June 2015 Vol.2 No.2 126-132

# Dental Radiology processing for abscess detection

SANCHEZ, María*†, MOLINAR, Jesús, VAZQUEZ, Sandra and ORDOÑEZ, Felipe

Received January 8, 2014; Accepted June 12, 2015

## Abstract

A reliable diagnosis of pathologies by dental professionals, requires specialized tools, mainly processing digital radiography. In this paper we present the development of a technique for detecting dental abscess by processing a radiological image, thus supporting dentists to make an accurate diagnosis of this pathology.

**Dental Radiology, Image Processing, Dentistry, Dental Abscesses Detection**

**Citation:** SANCHEZ, María, MOLINAR, Jesús, VAZQUEZ, Sandra and ORDOÑEZ, Felipe. Dental Radiology processing for abscess detection. ECORFAN Journal-Bolivia 2015, 2-2: 126-132

* Correspondence to Author (email: msanchez@itcg.edu.mx)
† Researcher contributing first author.

## Introduction

Currently in the age of digitization, numerous application areas are involved in digital image processing, in order to improve image quality for correct human interpretation or to facilitate the search for information. Dentistry is a science of health required for its diagnosis, digital x-ray images with good quality, as it is essential for making a good analysis of dental curing repair or replacement.

Digital radiography is a tool that facilitates and improves the quality of diagnosis of medical specialists, but it is still an expensive technology, which has unfortunately prevented from being used by most dentists specialists in Mexico. In the European Community and the USA 90% of dental specialists use digital equipment, while Mexico less than 10% use them.

The extra-oral imaging techniques, although used in conjunction with special projections have their limitations. The basic problem of the patient's exposure to radiation and the implications has prompted researchers to implement new techniques where exposure is limited, without affecting the quality of radiography and interpretations, and consequently the diagnosis.

Computer technology applied to the field of radiography has made the acquisition, handling, storage, transmission and enhancement of digital images possible.

Few investigations have been carried out for the detection of dental diseases by analyzing a radiographic image. Pereira [1], carried out an analysis with statistical tools of quality intraoral radiography.

A comparison of the information from dental radiography and CT with respect to the detection of lesions of endodontic and its relationship with its neighboring anatomical structures such as the mandibular canal is presented in [2]. A study to determine the diagnostic accuracy of Chargecoupled Devices (CCD) Photo Stimulable Phosphor (PSP) and radiography in the detection of cavities devices are disclosed in [3]. In [4] the authors propose a segmentation scheme of each tooth periapical radiographs and used for recognition of the teeth, Otsu thresholds and analysis of connected components and the delimitation of the teeth by monitoring limits and morphological operations. In [5] the authors developed a system of image analysis and dental X-ray diagnosis of tooth decay whor has anomalies. Segmentation has been done by applying the integral projection technique to remove the individual tooth and therefore the characteristics of tooth maps surface generated for analysis and detection process.

They have carried out some studies on segmentation and edge detection in images through Matlab. A system of recognition of a Latin American tropical fruit using computer vision techniques presented in [6]. In [7] it carried out an analysis of the operators to detect edges in images, to find some flaw in non-cylindrical glass containers by Matlab tool. In [8] have developed TecLines, a free Matlab-based layout to locate and quantify the guideline patterns from satellite data and digital elevation models (tectonic analysis).

This research considers the dental abscess pathology, because it is a dental disease that if is not treated early, can cause complications such as tooth loss, spread of infection to soft tissue, jaw and other areas of the body resulting in brain abscess, endocarditis, pneumonia or other complications [9].

ISSN-On line: 2410-4191


SANCHEZ, María, MOLINAR, Jesús, VAZQUEZ, Sandra and ORDOÑEZ, Felipe. Dental Radiology processing for abscess detection. ECORFAN Journal-Bolivia 2015.

Abscesses are detected in a dental radiographic image in order to facilitate the diagnosis to dental professionals.

This article is organized as follows: section 1, the theoretical foundation that supports this research is presented; in Section 2, the materials and methods used are detailed; in section 3, the results and discussion which has been reached in this work, and finally in section 4 disclosed the conclusions of the investigation.

**Theoretical basis**

**Digital Radiology**

Obtaining an X-ray is entering virgin radiography (X-ray sensitive) in the patient's mouth for that; a team that emits X-rays to activate the intraoral image plate is used. Subsequently the specialist obtained the radiation printing tooth by a developing process and fixing the image onto film measuring 3x2 cm. Once dry the radiography is mounted on a light panel and it works by monitoring the picture. Thereafter, having invested about 5 minutes based on the image it can continue to work on the damaged tooth.

Furthermore, digital technology makes a similar process that was described above is based on a (X-ray) sensor designed specially for dental use and the size of a radiograph. The X-ray equipment is the same, but now through the sensor with the interface hardware attached to it digital images that can be stored on a computer. The images of the teeth are obtained by extra-oral radiographic techniques. Among some of the new techniques extrabucl radiology are: Xerorradiografía, Zeugmatografía, Radiovisiography, Stereo-rradiografía, thermography [10]; each has its principle of operation, its advantages, disadvantages and use in the field of medicine.

Filmless X-rays or electronic imaging has an important impact in the dental field. Because the use of electronic images results in a decrease of the radiation dose to the patient was quickly accepted in dental practice. Furthermore, when is used these tools using chemical highly polluting the environment is avoided, because they are removed 100% waste substances, at a time were used to obtain intraoral radiography.

There are several methods for obtaining digital images. Some of them are [10]:

– Digital Conventional radiography using a flatbed scanner and transparency adapter.

– Digital Conventional radiography using a coupling device in the camera.

– Semi-direct digital image using photostimulable phosphor sheet.

– Direct digital image using a coupling device, metal semiconductor and other electronic devices.

Some of the advantages of digital radiography are [10]:

**Obtain immediate image.**

Do not require conventional film processing, process which can lead errors in product revealed poor handling of the developer substances.

– Automated Image Analysis.

– Storage of patient information.

– Teleradiology (image transfer to different places).

ISSN-On line: 2410-4191

- Education and patient interaction.

- Elimination or digital subtraction of background images and grayscale display in reverse, for example, the images appear radiolucent and radiopaque white black.

Some of the disadvantages of digital radiography are [10]:

- High cost, especially the panoramic systems.

- It requires lots of storage on the hard drive for images.

- In direct digital radiography, the sensor and the computer are directly connected, making the placement of intraoral level sensor to a difficult process.

- Loss of definition and image resolution when compared to conventional films when printed.

- The manipulation of the images may stray to other uses; in some systems the difficulty of simultaneously displaying multiple images (images of the entire oral cavity) occurs; printed images may be distorted with time.

- Legal ramifications - is questionable use of digital images as evidence during a trial, as they are manipulated images.

**Image Processing**

The image processing consists of a series of steps involving the improvement, restoration, analysis and in some cases, changes of digital images. Image processing aims to improve the look of them and make more evident in certain details that want to note.

The main objective is to improve the diagnosis more efficiently using the information contained therein. The main operations relating to image processing are enhancement, restoration, analysis, understanding and synthesis [10].

Within the image processing include: Pattern recognition, also called reading patterns, identifying shapes and shape recognition. Patterns are obtained from segmentation processes, feature extraction and description, where each object is represented by a collection of descriptors.

Pattern recognition is a primary part in some intelligent systems for decision-making, and is applicable in manufacturing tasks, visual inspection, medical diagnosis, speech recognition, etc. Depending surveyed different procedures for data analysis and classification algorithms are followed.

Morphological filters are able to influence image structures, previously designated by defining structural member. All morphological operations on images perform their function, using a structural element called reference structure [12].

Thresholding is a method that covers digital image segmentation and seeks a threshold value that allows binarizing the image, properly separating the background and the object to be separated. The main objective is to get the best T (threshold) right between the gray values into images that allow optimal separation between the object and the background value.

The erosion process refers to removing one layer of pixels in a structure.

ISSN-On line: 2410-4191

**Dental Diseases**

Among the most common dental diseases are: cavities, gingivitis, periodontitis, physical trauma (strokes) and dental abscess. A brief explanation of each [11] is as follows:

a) Gingivitis. It is involving inflammation of the gums caused by an infection (bacteria) or the accumulation of plaque and tartar. If not attended in time, it can affect the bone and become periodontitis.

b) Periodontitis. It is a progressive infection of the gums and bone loss around the tooth, causing the loosening of teeth.

c) Dental Caries. It is a multifactorial disease characterized by the destruction of tissues resulting from tooth demineralisation caused by acids generated by plaque bacteria. There are different types of decay: Interproximal caries, occlusal caries, Caries buccal or lingual, Recurrent Caries and Caries Horse.

d) Dental abscess. It is a collection of infected material (pus) in the center of a tooth due to a bacterial infection. A tooth abscess is a complication of tooth decay. It can also occur when a tooth is broken or chipped. Openings in the tooth enamel allow bacteria to infect the center of the tooth (the pulp). The infection can spread from the root of the tooth to the bone that support [3].

**Materials and methods**

For image processing was used Matlab, given the range of tools offered by the programming environment, with a primary focus on the toolbox: Image Acquisition and Image Processing, which are geared specifically for image processing.

A sample of ten dental digital imaging with the pathology of abscess was considered.

The image obtained from dental digital radiography is a grayscale image. Radiography is processed through several stages to perform detection of pathology.

The methodology for conducting the detection, is described below:

a) Preparation of the radiographic image in grayscale.

b) Thresholding. It was observed that the best value T after performing the histogram of the images to be treated is 90, a value that was used in this investigation. The resulting image is a binary image.

c) Erosion. Experimentally it was found that the size of the radius must magnitude 5 and the reference structure disk.

d) Determining patterns that distinguish one object from another. Measuring a set of properties within the different regions identified as objects in the binary image was performed. He carried out the calculation of the centroids for the connected components in the image. To do this, the regions previously were in the image and a matrix was obtained with different numbered tags that mark the existence of different objects in the image.

e) Mapping of external borders of the objects and the boundaries of the holes within objects. To perform this operation the bwboundaries function was used [13] Matlab.

f) Preparation of the object with more pixels.

g) To present the image to the detection of pathology.

ISSN-On line: 2410-4191

## Results and Discussion

In the previous section the methodology used for the detection of dental abscesses is described. In this section the results obtained after applying the methodology are shown.

Figures 1 and 2 show two cases of abscess detection investigated in this work. From the original image performs thresholding and erosion process, as shown in Figures 1 and 2 subsection b. Figures 1 and 2 paragraph c, show the labeling of the objects found in the image from a centroid, marked with an "*".

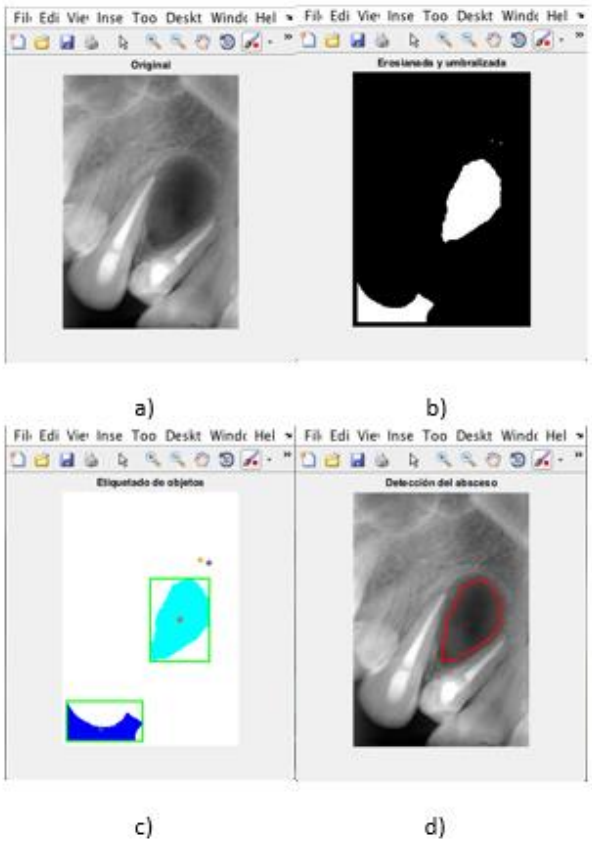


**Figure 1** Case 1 abscess detection. Image: a) Original, b) eroded and thresholded, c) labeling objects, d) Detection of the abscess.

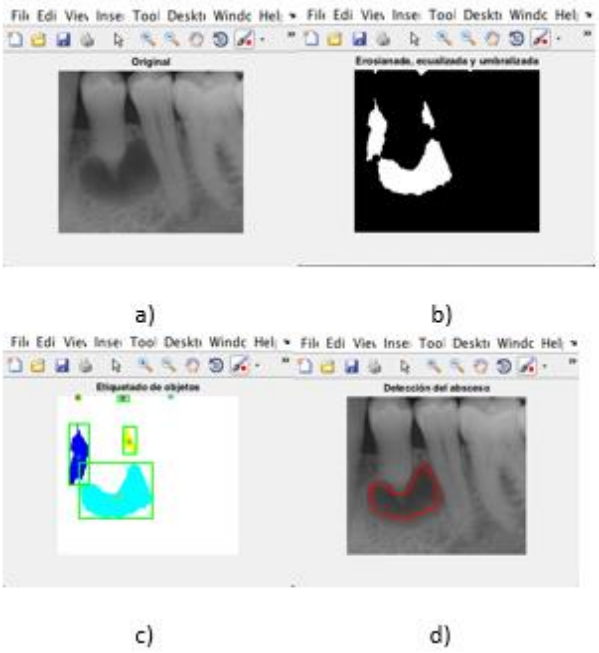


**Figure 2** Case 2 abscess detection. Image: a) Original, b) eroded and thresholded, c) labeling objects, d) Detection of the abscess.

Como puede observarse en las figuras 1 y 2 inciso d, se detecta claramente el absceso en las imágenes. Los resultados obtenidos en estas imágenes, fueron similares a los probados con otras imágenes y la misma patología.

## Conclusions

As a result of the investigation it is concluded that the development of a technique for detecting pathology abscess, facilitates the diagnosis of periapical abscesses to dental professionals by processing a dental X-ray image. In addition, the methodology is right for this type of pathology detection.

Future work will be performed analysis and more radiographic images and other diseases more accurately validate the detection technique employed in this work.

ISSN-On line: 2410-4191

**References**

Pereira Valbuena, E. G. Análisis radiográfico del grado de obliteración de la sutura palatina media como posible orientador en la estimación de la edad: diseño de estudio/Radiographic analysis of the obliteration of the mid-palatal suture as a possible point of orientation in the estimation of age: design for a study (Doctoral dissertation, Universidad Nacional de Colombia).

Velvart, P., Hecker, H., & Tillinger, G. (2001). Detection of the apical lesion and the mandibular canal in conventional radiography and computed tomography. Oral Surgery, Oral Medicine, Oral Pathology, Oral Radiology, and Endodontology, 92(6), 682-688.

Abesi, F., Mirshekar, A., Moudi, E., Seyedmajidi, M., Haghanifar, S., Haghighat, N., & Bijani, A. (2012). Diagnostic accuracy of digital and conventional radiography in the detection of non-cavitated approximal dental caries. Iranian Journal of Radiology, 9(1), 17.

Lin, P. L., Huang, P. Y., Huang, P. W., Hsu, H. C., & Chen, C. C. (2014). Teeth segmentation of dental periapical radiographs based on local singularity analysis. Computer methods and programs in biomedicine, 113(2), 433-445.

Rad, A. E., Amin, I. B. M., Rahim, M. S. M., & Kolivand, H. (2015). Computer-Aided Dental Caries Detection System from X-Ray Images. In Computational Intelligence in Information Systems (pp. 233-243). Springer International Publishing.

Montoya Holguin, C., Cortés Osorio, J. A., & Chaves Osorio, J. A. (2014). Sistema automático de reconocimiento de frutas basado en visión por computador. Ingeniare. Revista chilena de ingeniería, 22(4), 504-516.

Ruiz Flores, B., & Ullauri Ulloa, F. (2009). Detección de fallas en envases de vidrío no cilindricos utilizando localización de bordes mediante la herramienta de matlab.

Rahnama, M., & Gloaguen, R. (2014). Teclines: A matlab-based toolbox for tectonic lineament analysis from satellite images and dems, part 1: Line segment detection and extraction. Remote Sensing, 6(7), 5938-5958.

Marx, J., Walls, R., & Hockberger, R. (2013). Rosen's Emergency Medicine-Concepts and Clinical Practice. Elsevier Health Sciences.

Sikri, V.K. (2012). Fundamentos de Radiología Dental. Caracas-Venezuela: Amolca.

Olga A.C. Ibsen. (2014). Patología oral para el higienista dental. : ELSEVIER/Masson.

Cuevas, E., Zaldívar, D., & Pérez, M. (2010). Procesamiento digital de imágenes con MATLAB y Simulink. Alfaomega Ra-Ma (México).

Gonzalez, R. C., Woods, R. E., & Eddins, S. L. (2004). Digital image processing using MATLAB. Pearson Education India.

ISSN-On line: 2410-4191

Article ECORFAN Journal
NUTRITION June 2015 Vol.2 No.2 133-142

# Habits of consumption of fruits and vegetables in Mexican adolescents and their relationship with eating disorder

DÁVILA-LOAIZA, Martha Yolanda†

*Universidad de Londres*

Received January 8, 2014; Accepted June 12, 2015

## Abstract

This descriptive information intended to know the habits and preferences of some foods in Mexican adolescents, in addition to the benefits and barriers of adolescents to the consumption of fruits and vegetables and their association with overweight and obesity in adolescents. In the study of dietary patterns of the National Health and Nutrition Examination Survey, 2006 to 2012 and Survey teens to IMSS, dietary patterns were identified in Mexican adolescents. On the other hand the concern of the adolescent population fatten forces us to think about the influence of the prevailing aesthetic model in today's society and internalize it. It is known that concern about body weight is one of the variables of higher risk and can lead to disordered eating behavior. In short if the teen integrate within their usual diet group frutassegún vegetables and adequate intake recommendations, would help adolescents to have less weight and health problems, given the high percentage of water, fiber, low densidadenergética and contribution vitamins and minerals containing this group slowing in a sense the onset of eating disorder.

**Citation:** DÁVILA-LOAIZA, Martha Yolanda. Habits of consumption of fruits and vegetables in Mexican adolescents and their relationship with eating disorder. ECORFAN Journal-Bolivia 2015, 2-2: 133-142

† Researcher contributing first author.

## Introduction

### Adolescence

The word comes from the Latin adolescens is the active ingredient or present verb adolescere, it means to grow, to increase. Precisely liabilities and past participle of the same verb is adultus, which means "grown up" the already finished growing. The onset of adolescence has in the biological definition of sexual maturity (puberty), adolescent becomes an adult when it becomes financially and emotionally independent of their families. The World Health Organization (WHO) is an international organization that sets health policies in the countries and defines adolescence as the period population group between 10 and 19 years old. The group is between 15 and 24 defines it as youngsters. If we add the age groups between 10 and 24, they represent 30% of the total Latin American population.

Psychosocial development understand the process of progressive differentiation of the central nervous system that allows the acquisition of motor, language, cognitive and social empowering the individual to function normally within the family and society.

Classification of adolescence (Cecilia Silva 2007):

- Early (10-14 years old)
- Media (15-17 years old)
- Late and young adults (18-24 years old)

**Psychosocial development in early adolescence (10-14 years):**

**Independence**

- Lack of interest in family activity
- Changes in mood.

**Body Image**

- Importance of appearance
- Importance of fashion

**Adoption of new lifestyles**

They generally have friends of the same gender. Identity

The relationship with others helps them take their characteristics for the development of their personality; have fantasies, they need privacy, all of which is derived from a process of internal reflection we call cognitive thinking.

**Psychosocial development in middle adolescence (15 a 17 años) (Silva Cecilia 2007):**

**Independence**

- They have family conflicts
- Testing of the learned values.

**Body Image**

- Concern about appearance

**Adoption of new lifestyles**

- Sense of belonging or affinity groups or with their peers.
- We give great importance to the values of the group of friends.
- Begin heterosexual dating

ISSN-On line: 2410-4191

**Identity**

- Intellectual ability
- Shared Feelings.

**Psychosocial development in late adolescence (18-21 years and even up to 24 years) (Cecilia Silva 2007):**

**Independence**

- Acceptance of responsibility
- Acceptance of advice.

**Body Image**

- Acceptance of your image.

**Adoption of new lifestyles**

- Expanding your groups
- Using and managing your time.

**Identity**

**Manifest a vocation**

**Set realistic commitments.**

Accepted moral, religious and sexual values MEXICO adolescent population (ENSANUT 2012)

While there is a group of relatively healthy old who has already passed the critical stage of the mortality and morbidity of childhood, and still does not face the problems of adulthood, adolescents contribute more proportionally to their weight population health conditions that result from behaviors that compromise their present and future welfare.

By following the definition of the previous surveys and according to international consensus adolescents comprise individuals from 10-19 years old. During the teens 21519 ENSANUT which together accounted for 22,804,083 estimated as residents in Mexico in 2012. This population equivalent to 20.2% of the people in this country were interviewed. Of that total, 50.3% are men and 49.7% women, which show a trend of higher percentage of women, it believes that the ENSANUT 2006 the percentage was 49.2%. The size of the adolescent population represents a decrease of 0.3% in relation to the size of the group in 2006 ENSANUT.

**Eating disorders in adolescents (ENSANUT 2012)**

The proportion of adolescents (10-19 years) at risk of having an eating behavior disorder was 1.3% (1.9% in females and 0.8% in males).

The proportion of adolescents at risk of having an eating disorder was half a percentage point higher in 2012 ENSANUT recorded in 2006. The data reported in the ENSANUT 2012 (Gutierrez et al., 2012) showed that the frequently dietary risk behaviors among Mexican adolescents (10-19) years were: concerns about fat, eat too much and lose control over what you eat. In both sexes we found that fasting, dieting, taking pills, laxatives or diuretics in order to lose weight was the most frequent risk behavior.

When comparing age groups, males 14 to 19 years had a higher prevalence of risk behaviors, such as eating too much and exercising, that of 10-13 years.

Teenagers 14 to 19 years had a higher prevalence of all eating disorder (except induce vomiting) that adolescents aged 10 to 13 years.

ISSN-On line: 2410-4191

In the National Health Survey in school (ENSE (Shamma-Levy, 2010)) reports that preteens 10 years at 8% indicated a feeling of not being able to have control, to eat, and 0.7% practiced vomiting self-induced, 3% performing compensation practices such as fasting or excessive exercise with the intention to lose weight, just as 10% of schools had an inadequate eating behavior in the three months prior to implementation of the survey.

**Eating habits of adolescents.**

**Definition of terms**

Eating habits: set of behaviors acquired by an individual, by the repetition of acts in the selection, preparation and consumption of food. Healthy eating habits: eating behaviors repeat in which we bring a lot of energy and nutrients needed for our age and daily activity, sufficient to protect the nutritional needs (R. Tapia 2005).

**Feeding Adolescents Power**

Food in Mexico City varies according to socioeconomic strata. In particular the concept of health is related to the concerns of different groups in the upper strata has to do with nature and with different groups: in high strata has to do with the nature and care of the image, while in the lower strata associated with the health and satiety, as opposed to hunger.

Furthermore the modification of diet due to socio-cultural changes, from the internal point of view that is, in their homes individuals develop habits and food preferences and households choose their food mainly on the market, or convenience stores, given that they are no longer cultivated. Eating habits and nutrition of adolescents are affected by snacks or drinks they buy in schools or near them, as may prefer them over traditional foods prepared at home.

They tend to be more tasteless, less sweet and fatty foods preferring innovative product of globalization, like fast food.

Obviously, food prices are non-core, also shape or distort the election, as the public adjusts its tastes and cultural budget constraints preferences and seeks diets that are affordable, filling and satisfactory elsewhere, where industrialized foods fill a nutritional niche. Increasingly they offer basic food options as tortillas, breads and pastas.

Processed foods also provide concentrated through fat snack foods and sugars in sodas energy. We know that eating plenty of these products contribute to overweight, obesity and chronic diseases, and may also contribute to malnutrition, because it distracts the appetite that could lead to energy consumed through foods also provide other nutrients.

Lack of time is also a factor in the selection of food away from home; it may be that while adolescents face between an obligation and other students to choose the products they sell in the shop, you get and consume more quickly, rather than a more nutritious food, such as those that have only an hour for power; in these conditions, acquisition, preparation, consumption and cleanup are time constraints that severely reduce the nutritious options. The work schedule interferes with parent family meals, with traditional communication and healthy eating habits, with pleasure and sociability to food and nutrition and individual health generational? Does it happen in Mexico that specific meals throughout the day are spacing?

**Macronutrient intake in teens**

In a survey of adolescents (10-14años), all beneficiaries of the Mexican Social Security Institute (IMSS).

ISSN-On line: 2410-4191

The consumption of sweets, soft drinks, juices and pastries was 30.1, 27.1, 21.1 and 13.8%, while teenagers 15 to 19 years the percentages were in the same order, 30.3, 28.6, 20.2 and 12.5%. (Jimenez Cruz, et al 2002)

The information provided in the National Youth Survey 2005 (Perichart O. Pereda, 2007) tells us that 29% of adolescents 12 to 14 years taking soft drinks daily, 30% ate sweet snacks, salty snacks 24% and 11% consuming calls "fast food"; in adolescents aged 15 to 19 were observed frequencies of 36.0, 24.4, 23.5 and 120% according to the same order.

In the same sense teens in California in ninth grade the frequency of consumption of fruits is at least two servings of fruit per day was 20% and eating at least three servings of vegetables was 47% and IMSS beneficiaries of the study (Flores Huerta S, et al 2006) in the group of 10 to 14 years 35.7% of the subjects reported consuming fruit daily and 19.1% consumed vegetables; among 15- to 19 frequencies consumption of these foods was 35.0 and 20.4%, respectively.

**Barriers and Benefits of consumption of fruits and vegetables**

Given the benefits of eating fruits and vegetables it is important to identify factors that motivate or impede such consumption, especially in adolescence. Studies on this subject have been based on the Transtheoretical Model of Prochaska, particularly on the pros and cons (Di Noia, et al., 2006)

There is little research on the consumption of fruits and vegetables by adolescents. These studies carried out on samples of developed countries, they showed no difference in the perceived benefits by gender.

Men think it gives them more energy while women favoring their physical appearance; another group said that fruits and vegetables are healthy foods that improve school performance, physical fitness and self-esteem. (Di Noia, et al., 2006).

Other research that considers the theoretical constructs of benefits and barriers, focus healthy eating behavior in the adult population. (López-Azpiazu I. et al., 1999).

Also in Mexico in the northern states of the republic (Matamoros Tamaulipas), among which is Tamaulipas, they are characterized by low consumption of fruits and vegetables; no published studies documenting exactly the benefits and barriers perceived by adolescents to include these foods in their diet and this issue has not been explored in Mexican adolescent population. For both a scale is used to determine benefits and barriers for adolescents to the consumption of fruits and vegetables they vary according to gender.

The main benefit for the consumption of fruits and vegetables for males was "take care of my health by eating fruits and vegetables" and the female was "I like the taste of fruits and vegetables."

The benefit with the lowest score was the fact that consumption of fruits and vegetables help to have a lower chance of developing cancer, a finding that is consistent in other studies have reported that the population does not identify long-term benefits of eating fruits and vegetables or consumption of healthy eating. (Di Noia J, 2006).

Regarding barriers to eating food aspects they have been identified as the availability of less healthy foods and they are prepared easier and faster besides flavor.

ISSN-On line: 2410-4191

Likewise, regardless of the gender adolescents they mentioned that lack of support from parents to follow a healthy diet because it is they who buy food and that their parents are not role models.

Furthermore the findings of this study indicate that the perceived benefits and barriers for behavior can be influenced by personal factors, as in the present study according to gender differences were found. For example, women receive greater benefits than men, some authors suggest that men prefer foods like meats and hard to digest foods (Paquette MC 2005) and (Lupton D. 1996).

With regard to the barriers to healthy food consumption aspects have been identified as the availability of less healthy foods and they are prepared faster and easier, besides flavor. Likewise, regardless of the gender adolescents they mentioned that lack of parental support to follow a healthy diet because it is they who buy food and that their parents are not role models.

**Recommendation of Vegetable and fruit in the adolescent population (NOM-043-SSA1-2012)) (Social Welfare Guidelines DOF)**

It should be informed that during this growth stage, which should be monitored as the Mexican Official Standard NOM-031-SSA2-1999 points, to care for the child's health, so you should adjust the suggested amount of diet accelerates correct, according to the familiar availability and physical activity, particularly in the supply of iron, calcium and folic acid and dietary fiber.

Source of iron foods of animal origin, legumes and vegetables.

Source of calcium: cereals, animal foods mainly.

Source of folic acid food of animal origin, vegetables, fruits and cereals.

Source of dietary fiber. Cereals, vegetables, fruits and legumes is

In food safety as nutritional quality criteria for food assistance program includes subjects Vulnerable risk groups subject to food assistance, are preferably children and adolescents, pregnant women, nursing mothers, people with disabilities, vulnerable seniors income. (DOF 06/10/2013 guidelines)

The corresponding food support for this program to be one of the following options:

a) Provision, if required, can be accompanied by Food complement.

b) Breakfast or hot meal according to the criteria of nutritional quality

**Purse**

Include 4 or more staples that constitute part of the food culture of the beneficiaries.

Include at least two or three food groups mentioned in the (NOM-043-SSA2-2012) vegetables and fruits, cereals, legumes and animal foods.

Include at least 2 cereals are a source of dietary fiber.

Include at least 2 varieties of legumes.

Should include a supplement, it should not contain sugar or sweeteners from their first three ingredients.

Breakfast or hot meal and / or cold mode; Quality Criteria (VF)

ISSN-On line: 2410-4191

The same criteria for specific nutritional quality for school breakfast or lunch mode are considered hot. It is recommended:

20 cyclical school breakfast menus Committees whose design must consider the following points:

Include skim milk and / or natural water:

Should include fruit shall include the following: be prepared with only natural fruit, add a maximum of 20g / L ie 2 tablespoons per liter, this should be low frequency.

Include a main dish including vegetables, whole grains and legumes or animal food. That is fat dishes that require no or very small amounts, as sauce stewed, roasted, baked, roasted or cooked.

In order to contribute to increased consumption of vegetables, onion, garlic and tomato collection and / or tomatillo, will not be taken into account as a serving of vegetables.

Promote the serving of fruit or vegetable is fresh, based on purchasing power and distribution DIF parent or school breakfasts for purchase committees.

Offer fresh fruit or dried at breakfast cold mode.

On the recommendation of the group of fruits and vegetables raw or cooked grams for school-teen population.

| | | | |
|---|---|---|---|
| Vegetables and fruit | Garlic, onion and other vegetables parsley cilantro to season | To Taste | |
| | VEGETABLES | 100g | |
| | Leafy vegetables | 50g | |
| | Chopped vegetables to accompany rice, soups or stews | 50g | |
| | Guava, apricot plum | 80g | 2 pieces |
| | Banana, apple, pear, orange, tangerine | 80g | ½ parts |
| | Watermelon, melon, pineapple | 80g | ½ cup |

Guidelines of the Social Food Assistance Strategy 2015. (Ministry of Health, DIF)

Finally to determine calorie needs is taken into account calorie per unit of height for age and sex (kcal / cm). The maximum caloric intake of women is about 2550 kcal during the time of menarche, around 12 years. This peak demand is followed by a gradual reduction. Parallel caloric intake of men occurs during the peak of the growth spurt and progressively increases to 3400kcal at age 16 and then decrease in proportion of 500 kcal to 19 years. Whose energy distribution percentage is 12-15% protein, 20-30% fat and 55-60% carbohydrate.

In the same period as mentioned before needs increase vitamins (B vitamins) and minerals (zinc, calcium, iron, folic acid), whose sources come from vegetables and fruits and other foods.

**Fruit and vegetables intake in Mexican population (Ramirez-Silva et al., 2009)**

The variables that are taken into account the recommendation of vegetables and fruit (VF), dietary intake (g) adequacy percentage (percentage of total consumption of the population or half the amount of the recommendations by the World Health Organization (WHO) and (AHA) American Heart Association.

Defining fruit and vegetables under the name of diversity of plant foods, vegetables, roots, leaves, stems, seeds, inflorescences, flowers and bulbs that contribute to the regulatory function of the body, they provide vitamins and minerals, provide much of the water and fiber the body needs. They are consumed raw or cooked, and have a low energy density and other bioactive components.

ISSN-On line: 2410-4191

Fruit juices are excluded due to the high fructose and energy and low in fiber is therefore considered a negative effect on health.

According to NOM-043-SSA1-2015 criteria dietary guidance, foods are classified into 3 groups food groups:

a) Vegetables and Fruits (VF)

b) ANIMAL

It should promote the consumption of fruits and vegetables and regional station, if is possible raw shell that incorporate them into the daily diet helps reduce the energy density of the diet, and they are a source of carotenes, vitamin A and C, folic acid and dietary fiber and give color and texture to dishes as well as other vitamins and inorganic nutrients.

Daily intake (DI) of VF is estimated intake in grams per day based on frequency of use. This consumption is expressed in grams and no calorie. The percentage of adjustment was made taking into account recommendations to prevent cardiovascular disease by WHO and AHA.

The recommended intake is 200g for 1-4 years, 5-8 years of 300g to 400g for people age between 9-59 years old. The classification is given in three categories according to age-specific intake;

Or above the percentage of recommended intake or adequacy or higher:

1) Adequate intake.

2) Moderate intake inadequate: from 50% to 90% of the recommended intake.

3) Inadequate intake elevadamente: less than 50% of the recommended or less than 50% adequacy intake.

Relate to fruit and vegetable intake were taken into account by categorizing regions of Mexico, which was divided four regions:

a) North (including North and South Baja California, Coahuila, Chihuahua, Durango, Nuevo Leon, Sonora and Tamaulipas)

b) Center (Aguascalientes, Colima, Guanajuato, Jalisco, Estado de México, Michoacán, Morelos, Nayarit, Querétaro, San Luis Potosí, Sinaloa, Zacatecas).

c) México City

d) South (Campeche, Chiapas, Guerrero, Hidalgo, Oaxaca, Puebla, Quintana Roo, Tabasco, Tlaxcala, Veracruz y Yucatán)

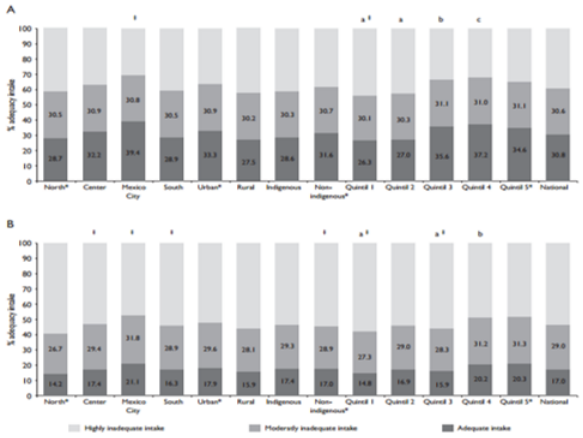


**Figure 1** Adolescents and adults adequacy percentage distribution according to the recommendation of intake of vegetables and fruits (VF), ENSANUT 2006.

The results analyzed are a total of 3224 children aged 1-4 years, 8,294 children 5-11 years old and 7722 adolescents aged 12-18 years and 16349 adults 19-59 years of age accounted for:

With 61.3 g vs. 26.2 g preschoolers, 68.9g vs.34.2g school children, adolescents .43.3g vs 72.9g and 65.8g vs. 56.8g adults respectively.

ISSN-On line: 2410-4191

The total amount of VF and recommended intake for each group is below the recommendation. See Fig. 1.

This study represents a low intake of fruit and vegetables among the Mexican population in relation to international recommendations. Low intake was observed in fruits and vegetables and in all age groups, regions, ethnic groups, higher socioeconomic levels in rural and urban population and both sexes. Only 30.8% of preschoolers, 17.0% from children of school age, 19.2% of adolescents and 24.2% of the adult population meets the recommended intake. Given the low intake in both low and high demand given the low socioeconomic levels, high prices of fruits and vegetables for calorie foods relative density low energy- and other cultural reasons linked to poverty. Another potential reason the population is poor access problems due to limitations of the transport of perishable foods such as fruits and vegetables.

At the same time the relationship with people living in northern given consumption patterns resulting from the nutrition transition due to globalization and modernization, in addition to weather conditions, which lavf staying indoors conditioners raising its price. The same relationship is associated in rural areas among indigenous people located in isolated areas whose local production compensates for the lack of supply in certain seasons of fruits and vegetables in season. And reinforcing the above low intake of certain groups is possibly related to demand rather than supply.

Definitely intake of fruits and vegetables among adolescents living in rural areas and non-indigenous is higher than in urban areas given the dietary patterns associated with modernity of life, for example eating fast food at home and abroad.

As a final conclusion is substantial efforts of parents, teachers, schools, teaching early childhood habits of healthy eating integrating the three groups of food diet as NOM-043 provides in particular VF, based on the recommendations by age in Suitable models settling sum power of parents to teenagers, who are subject to receive influence of the environment, accompanying the values of body image, whose value is overstated in this age also is up to the parent to provide a fair assessment of this to teenager, to prevent the occurrence of conduct disorder at an early age accompanied by physical activity according to age and skill adolescents.

**References**

Castillo Gerardo (2001),” Los Adolescentes y los problemas”, Editorial Minos México pág. 65

Di Noai J, Schinke SP, Prochaska J.O, Contento IR (2002), Application of the transtheoretical model to fruit and vegetable comsumption among economically disadvantaged African-American adolescents; preliminary findings. Am. J Health Promot. May-Jun; 20(5):342-8

Encuesta Nacional de Salud y Nutrición 2006 (ENSANUT 2006), INSTITUTO DE SALUD PÚBLICA MÉXICO.

Flores Huerta S, Acosta Cázares B, Rendón Macías ME, Klünder Klünder, Gutiérrez-Trujillo g, (2006). ENCOPREVENIMSS 2004 4, “Consumo de alimentos saludables o con riesgo parala salud, Rev Med Inst Mex Seguro Soc: 44: S63 78.

Gutiérrez J. P., Rivera Dammarco, J., Shamah-Levy, T. Villalpando-Hernández S., et al., (2012). Encuesta Nacional de Salud y Nutrición 2012. Resultados Nacionales. Cuernavaca, México: Instituto Nacional de Salud Pública

ISSN-On line: 2410-4191

Jiménez Cruz A., Bacardí Gascón M, Jones EG. (2002) Consumption of fruits, vegetables, soft drinks, and high fat containing snacks among Mexican children on the Mexico, U.S. border Arch Med Res ; 33:74 80

Lineamientos para dictaminar y dar seguimiento a los programas derivados del Plan Nacional de Desarrollo 2013-2018. Publicados DOF 10-06-2013.

López- Azpiazu I, Martínez-Gónzalez MA. Kearney J, Gibney M., Martinez JA. (1999), Percieved barriers of, and benefits to, healthy eating reported by spanish national simple. Public Health Nutr.Jun: 2(2):209-151.

Lupton D. Food, (1996). The body and the self, London, England: Sage

NORMA Oficial Mexicana NOM-043-SSA2-2012, Servicios básicos de salud. Promoción y educación para la salud en materia alimentaria. Criterios para brindar orientación.DOF-22-02-2013

Paquette MC, (2005) Perceptions of healthy eating: state of knowledge and research gaps. Can J Public Health, Jul-Aug; 96Suppl 3:S15-9, S16.

Perichart Pereda O, Balas Nakas M, Schiffman Selechnlk E, Barbato Dorsal A., Valdillo-Ortega F. (2007), "Obesity increases metabolic syndrome risk factors in school aged children from an urbanschool in Mexico city, J Am Diet Assoc: 107: 81 91.

Ramírez-Silva I., Rivera Dammarco J.,Ponce Xóchitl, Hernández-Ávila Mauricio, (2009) Consumo de frutas y verduras en la población mexicana: resultados en la Encuesta Nacional de Salud y Nutrición 2006, Salud Pública Mex ;51 supl4:SS74-S585.

Silva Cecilia (2007), "Como prevenir, detector y qué hacer si se presentan Trastornos Alimentarios". Editorial Pax México.

Tapia R. Norma Oficial Mexicana NOM-043SSA2-2005, servicios básicos de salud. Promoción y educación para la salud en materia alimentaria. Criterios para brindar orientación. (En línea) (Citado 6-Mayo 2015) 1-23 Disponible en: http:/www.censida.salud.gob.mx/descarga/ética/reglamento.pdf

ISSN-On line: 2410-4191

# Instructions for authors

A. Submission of papers to the areas of analysis and modeling problems in the areas of Engineering, Chemestry, Optical, Resources, Food Technology, Anatomy and Nutrition.

B. The edition of the paper should meet the following characteristics:

-Written in English. It is mandatory to submit the title and abstract as well as keywords. Indicating the institution of affiliation of each author, email and full postal address and identify the researcher and the first author is responsible for communication to the editor

-Pretexting Times New Roman #12 (shares-Bold) and italic (subtitles-Bold) # 12 (text) and #9 (in quotes foot notes), justified in Word format. With margins 2 cm by 2 cm left-right and 2 cm by 2 cm Top-Bottom. With 2-column format.

-Use Calibre Math typography (in equations), with subsequent numbering and alignment right: Example;

$$\sigma\epsilon\sum:H\sigma=\bigcap\_(s<\sigma)Hs \quad (1)$$

-Start with an introduction that explains the issue and end with a concluding section.

- Items are reviewed by members of the Editorial Committee and two anonymous. The ruling is final in all cases. After notification of the acceptance or rejection of a job, final acceptance will be subject to compliance with changes in style, form and content that the publisher has informed the authors. The authors are responsible for the content of the work and the correct use of the references cited in them. The journal reserves the right to make editorial changes required to adapt the text to our editorial policy.

C. Items can be prepared by self or sponsored by educational institutions and business. The manuscript assessment process will comprise no more than twenty days from the date of receipt.

D. The identification of authorship should appearing a first page only removable in order to ensure that the selection process is anonymous.

E. Charts, graphs and figures support must meet the following:

-Should be self-explanatory (without resorting to text for understanding), not including abbreviations, clearly indicating the title and reference source with reference down with left alignment number 9 with bold typography.

-All material swill support grayscale and maximum size of8cmwide by23cmtallor less size, and contain all content editable.

- Tables should be simple and present relevant information. Prototype;

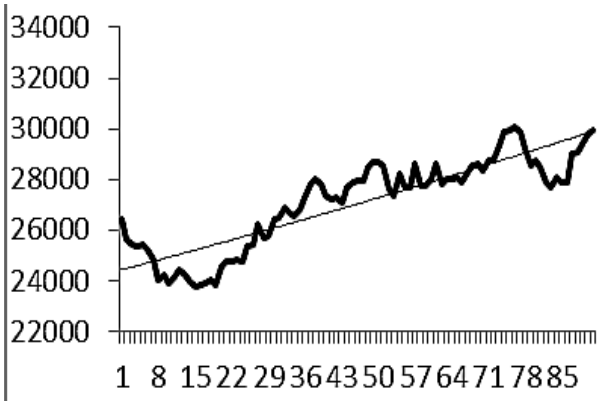


**Graph 1. Stochastic versus deterministic trend**

F. References are included at the end of the document, all its components will be separated by a comma and must the following order:

- Articles: Kejun, Z. (2012). Feedback Control Methods for a New Hyperchaotic System. Journal of Information & Computational Science, No.9. Pp :231-237.

- Books: Barnsley, M. (1993). Fractals Everywhere. Academic Press. San Diego.

- WEB Resources: http://www.worldfederationofexchanges.com, see: (August, 16-2012)

The list of references should correspond to the citations in the document.

G. The notes to footnotes, which should be used and only to provide essential information.

H. Upon acceptance of the article in its final version, the magazine tests sent to the author for review. ECORFAN only accept the correction of typos and errors or omissions from the process of editing the journal fully reserving copyright and dissemination of content. Not acceptable deletions, substitutions or additions which alter the formation of the article. The author will have a maximum of 10 calendar days for the review. Otherwise, it is considered that the author (s) is (are) in accordance with the changes made.

I. Append formats Originality and Authorization, identifying the article, author (s) and the signature, so it is understood that this article is not running for simultaneous publication in other journals or publishing organs.

**Sucre-Bolivia ____ , ____ 20_____**

## Originality Format

I understand and agree that the results are final dictamination so authors must sign before starting the peer review process to claim originality of the next work.

_____

Article

_____

Signature

_____

Name

**Sucre-Bolivia ____ , ____ 20_____**

## Authorization form

I understand and accept that the results of evaluation are inappealable. If my article is accepted for publication, I authorize ECORFAN to reproduce it in electronic data bases, reprints, anthologies or any other media in order to reach a wider audience.

_____

Article

_____

Signature

_____

Name

## Engineering

"Calculation of Dynamic Properties of Hybrid Supports of injected lubricant. Analytical Development"
RAMIREZ, Ignacio, JARAMILLO, Jesús y RECIO-CAMPOS, Celeste
*Instituto Tecnológico de Pachuca.*

## Chemestry

"Location Effect of Temperature Control on the Fund in a CPD"
MEDINA, Leonardo, URREA, Galo, REYNOSO, Eusebio and PLIEGO, Yolanda
*Instituto Tecnológico de Orizaba*

## Optical

"Portable system for capturing images of the sclera"
ROJAS, Carlos, ROJAS, Rafael, BAUTISTA, Jorge y TRUJILLO, Valentín

## Resources

"The method of small perturbations to Calculate Stiffness and damping in a Short Chumacera"
RAMIREZ, Ignacio, CANO, Alexis and ANTONIO, Alberto
*Instituto Tecnológico de Pachuca.*
*Universidad Tecnológica de la Mixteca*

## Food Technology

"Evaluation of antibacterial activity of essential oil Origanum vulgare (oregano)"
SANDOVAL, Francisca, DOMINGUEZ, Maricela, CONTRERAS, Raúl and REYES, Coral

## Anatomy

"Dental Radiology processing for abscess detection"
SANCHEZ, María, MOLINAR, Jesús, VAZQUEZ, Sandra and ORDOÑEZ, Felipe

## Nutrition

"Habits of consumption of fruits and vegetables in Mexican adolescents and their relationship with eating disorder"
DÁVILA-LOAIZA, Martha Yolanda
*Universidad de Londres*

ISSN-On line: 2410-4191